Stress-dependent permeability and fluid flow through parallel joints

Leonid N. Germanovich
School of Civil and Environmental Engineering, Georgia Institute of Technology, Atlanta, Georgia, USA

Dmitriy K. Astakhov
Pinnacle Technologies, Inc., Bakersfield, California, USA

Received 1 August 2002; revised 8 August 2003; accepted 7 May 2003; published 9 September 2004.

[1] It is well known that the permeability of a set of joints can significantly vary in response to in situ stress conditions and pressure of the flowing fluid. Frequently, joint sets are closely spaced, and although joint mechanical interaction could significantly affect their aperture, the interaction is usually ignored in the fluid flow models. It is rather obvious that this approach corresponds to the upper bound for flow rate and rock permeability. By taking into account the interaction between the joints, we show that modeling a joint set by an infinite array provides the lower bound. The difference between these bounds, however, can be rather large, so they may not always be used with the sufficient accuracy. From the conceptual standpoint, it is often tempting to model a set with a finite number of joints by an infinite array. The results obtained in this work clearly demonstrate that such a model may result in a significant underestimation (by orders of magnitude) of both the permeability and flow rate. Similarly, the assumption of noninteracting joints may significantly overestimate (also by orders of magnitude) the stress-dependent permeability and flow rate compared to those computed more accurately when accounting for joint interaction. Because the internal pressure can, in fact, close the pressurized joints while two edge joints (end-members) in the set remain widely open (since they are not suppressed from one side by the adjacent joints), unless the number of joints in the set is exceedingly large (typically, $>10^3$), the fluid flow through the joint set becomes highly heterogeneous, focusing in the edge joints. As a result, the permeability/flow rate dependence on the joint spacing is not monotonic but has a maximum and a minimum. The derived closed-form expression for flow rate/permeability ratio is asymptotically accurate and allows computations for rather arbitrary joint sets. *INDEX TERMS:* 5104 Physical Properties of Rocks: Fracture and flow; 5114 Physical Properties of Rocks: Permeability and porosity; 5139 Physical Properties of Rocks: Transport properties; 8010 Structural Geology: Fractures and faults; 8020 Structural Geology: Mechanics; *KEYWORDS:* joint sets, fluid flow, pressure, crack interaction, fracture apertures, stress-dependent permeability

Citation: Germanovich, L. N., and D. K. Astakhov (2004), Stress-dependent permeability and fluid flow through parallel joints, *J. Geophys. Res.*, *109*, B09203, doi:10.1029/2002JB002133.

1. Introduction

[2] It is well known that the permeability of a set of joints can significantly vary in response to several factors. Chemical precipitation from the solution can reduce [e.g., *Lowell et al.*, 1993] and even completely shut down [e.g., *Martin and Lowell*, 2000] rock permeability, resulting, for example, in a set of mineralized veins [e.g., *Vermilye and Scholz*, 1995] instead of open fractures. Thermal expansion (contraction) also drastically affects permeability distribution and fluid flow characteristics [see, e.g., *Germanovich and Lowell*, 1992; *Lowell and Germanovich*, 1995; *Germanovich et al.*, 2000, 2001, and references therein]. The effect of confining pressure on permeability has been studied extensively both theoretically [e.g., *Gangi*, 1978; *Neuzil and Tracy*, 1981; *Tsang and Witherspoon*, 1981; *Walsh*, 1981; *Gavrilenko and Gueguen*, 1989] and experimentally [e.g., *Jones*, 1975; *Kranz et al.*, 1979; *Raven and Gale*, 1985]. If the pressure inside joints is sufficiently high for their growth [*Engelder and Oertel*, 1985; *Engelder and Lacazette*, 1990; *Srivastava and Engelder*, 1991], it may cause an appreciable permeability increase by enhancing the interconnectivity of joint sets. In the case of sparsely located fractures, for a given pressure and geometry, larger fracture size generally corresponds to a greater aperture. Hence it may appear that this is an additional reason to expect the permeability to increase in the set of growing joints. As shown in this paper, however, this expectation is not justified for closely spaced joints.

[3] If the fluid pressure inside the joints is not sufficient for their propagation, it can still affect the permeability of

Copyright 2004 by the American Geophysical Union.
0148-0227/04/2002JB002133$09.00

Figure 1. A set of parallel joints in the alternating siltstone and shale beds on the Appalachian Plateau near Finger Lakes, central New York (courtesy of Bruce Carter; see also *Helgeson and Aydin* [1991] and *Engelder et al.* [1999]).

the joint set by changing the apertures of individual joints. This mechanism is the basis of most models of stress-dependent permeability of fractured rocks. Such models are usually based on the concept of single, noninteracting fractures [e.g., *Gangi*, 1978; *Tsang and Witherspoon*, 1981; *Gavrilenko and Gueguen*, 1989; *David*, 1993]. It has been recognized only recently [*Nolte*, 1987; *Germanovich et al.*, 1998; *Bai et al.*, 2000] that joint elastic interaction can also become an important factor affecting layered rock permeability and fluid flow distribution.

[4] In this work, we study the effect of the elastic interaction of joints on stress-dependent permeability and fluid flow in jointed rock (Figure 1). We consider the dimensionless spacing, $s = b/(2c)$ (Figure 2a), that varies in the range of 10^{-2} to 10, which likely covers all the observed values of spacings reported in the literature (see, e.g., the review in the paper of *Germanovich and Astakhov* [2004]). Following *Germanovich et al.* [1998], *Germanovich and Astakhov* [2004] showed that it is not only necessary to take into account the interaction between the joints if $s < 1$, but also that for $s \leq 0.1$, which is not unusual (e.g., see Figure 1), joints can be closed by the fluid injection. In this paper, we show that for frequently observed joint sets with a spacing between 0.1 and 1, the conventional permeability estimates based on mapping joint density and their dimensions (size and aperture) may have to be reduced by at least one or two orders of magnitude. Even more importantly, we show that in contrast to the case of noninteracting joints, interaction of pressurized joints results in the redistribution of the fluid flow, which becomes highly nonuniform, concentrating (focusing) in the edges (end-members) of the joint set.

[5] To reduce the number of parameters and to emphasize the effect of joint interaction, we address the extreme case by ignoring the initial joint apertures and assuming that each joint opens because of the pressure applied to its sides and remote stresses acting far from the joint set. The initial joint apertures can be taken into account in the manner described by *Germanovich and Lowell* [1992, 1995] and a separate paper will be devoted to this case. In this paper, we follow the notations of *Germanovich and Astakhov* [2004], so that the terms "joint," "fracture," and "crack" are identical and we use the term "opening" (as a noun) in a generic sense. Further, the term "aperture" is synonymous to "displacement discontinuity" in Fracture Mechanics and should be distinguished from the "opening displacement" (i.e., crack side displacement), which characterizes the deformed shape of a loaded (e.g., pressurized) joint. If otherwise not indicated, the term "aperture" refers to the joint width at the center, e.g., $W = W(0)$ rather than $W(x)$ (see Figure 2b).

2. Permeability of a Set of Joints

[6] Following others [e.g., *Ji and Saruwatari*, 1998; *Bai et al.*, 2000], we consider the case of equally spaced joints of equal size (Figure 2a). Fluid flow through each joint can be calculated by employing the parallel flow (lubrication) approximation [e.g., *Bird et al.*, 1987]. For joints that are thin and smooth everywhere (except, perhaps, at their tips), the fluid flow, dq, along each joint increment, dx, can be considered as the flow between two parallel plates (Figure 2b):

$$dq = -\frac{2W_*^3}{3\eta}\left(\frac{W}{2W_*}\right)^{\gamma}\frac{\partial p}{\partial z}dx, \tag{1}$$

where $W(x)$ is the local joint aperture, η is the dynamic viscosity of the fluid, $\partial p/\partial z$ is the pressure gradient along

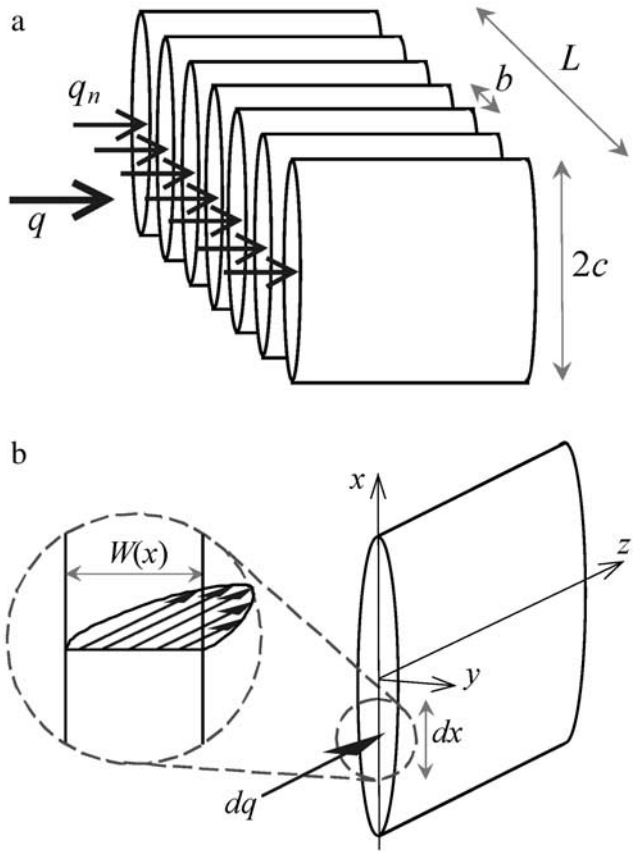

Figure 2. (a) A set of parallel, equally sized and spaced joints and (b) parallel flow (lubrication) approximation.

Table 1. Symbol Definitions

Symbol	Definition
	Roman Symbols
b	distance between joints (Figure 2a)
b_m	average spacing in the set of unevenly spaced joints (Figure 13)
c	joint half-size (Figure 2a)
c_m	mean joint half-size in the set of joints of different dimensions (Figure 13)
E	Young's modulus
$E_1 = E/(1 - \nu^2)$	plane strain elastic modulus
f	normalized flow (16) in the end-member joints
k	permeability
k_0	permeability in the model of non-interacting joints
$k_\infty = k_\infty(s)$	permeability of the infinite array of (interacting) joints
$L = (N - 1)b$	size of the set of N joints (Figure 2a)
m	exponent in the power-law model of non-Newtonian fluid
N	number of joints in a set
p	net pressure inside joints
q	total fluid flow rate
q_0	total flow rate in the model of non-interacting joints
$q_\infty(s)$	flow rate through one joint in the infinite array
$q_n(N, s)$	fluid flow rate in the nth joint in the set of N joints
$s = b/(2c)$	normalized joint spacing
s_{cr}	critical joint spacing at which joint sides touch
$s_m = b_m/(2c_m)$	mean normalized joint spacing in the set of unevenly spaced joints (Figure 13)
$W(x)$	displacement discontinuity or aperture
$W_0(x)$	aperture of a single joint (i.e., in the model of non-interacting joints)
$W_0 = W_0(0)$	aperture of a single joint in the middle
$W_n(x)$	aperture of the nth joint
$W_n(x, N, s)$	same
$W_n = W_n(0)$	aperture of the nth joint in the middle
$W_c = W_c(0)$	aperture of the central joint in the set in the middle point
$W_c(x)$	aperture of the central joint in the joint set
$W_c(x, N, s)$	same
$W_\infty(x)$	joint aperture in the infinite array
$W_\infty(x, s)$	same
$W_\infty = W_\infty(0)$	aperture of a joint in the infinite array in the middle
x, y, z	coordinate system aligned with the joint (Figure 2)
	Greek Symbols
$\delta = (W_c - W_\infty)/W_c$	relative error of modeling the joint set by an infinite array
$\delta_1 = (\chi_1 - \chi)/\chi$	relative error of the three-fracture model for the normalized flow rate
$\delta_2 = (\chi_2 - \chi)/\chi$	relative error of approximating χ by χ_2
γ	exponent in the generalized parallel flow approximation (1)
$\gamma = 3$	same in the case of the cubic law
η	dynamic viscosity of fluid
η_0	consistency index in the power-law model of non-Newtonian fluid
κ	fluid flow ratio or permeability ratio
κ_{max} , κ_{min}	upper and lower limits of fluid flow/permeability ratio, κ
κ_N	fluid flow/permeability ratio for a set of N joints
κ_∞	fluid flow ratio or permeability ratio in the model of infinite array
ν	Poisson's ratio
$\chi = (1/s)q_\infty(s)/q_\infty(1)$	normalized volumetric flow rate in the infinite array
$\chi_1 = (1/s)q_2(3, s)/q_2(3, 1)$	normalized flow rate approximated based on the three-fracture model
$\chi_2 = (1/s)q_2(3, s)/q_\infty(1)$	same as χ_1 but using $q_\infty(1)$ for normalization

the joint set (see the coordinate set shown in Figure 2b), W_* is the known parameter of the dimension of length (resulting from the deviation from the cubic law; see below), and p is the net or excess pressure, which is the difference between the actual fluid pressure in the joint and the remote stress perpendicular to the joint [see, e.g., *Germanovich and Astakhov*, 2004, Figure 2b]. All main parameters are listed in Table 1.

[7] In the case of Newtonian fluid, $\gamma = 3$ in equation (1). As suggested for fractures with multiscale asperities [*Pyrak-Nolte et al.*, 1988; *Sisavath and Zimmerman*, 2000] and/or contacting sides [*Oron and Berkowitz*, 1998], it could be more appropriate to increase the exponent, γ, in equation (1). Nevertheless, the cubic law ($\gamma = 3$) has been experimentally demonstrated for fracture apertures larger than 4 μm and for various rock types [*Witherspoon et al.*, 1980]. Furthermore, the cubic law can be successfully used for the flow between nonparallel surfaces if the aperture is harmonically averaged and the tortuosity of the flow path is included in the calculation of the pressure gradient [*Waite et al.*, 1999]. Also, in the case of the fluid flow through the open fracture segments considered in this work, the cubic law provides a leading order approximation for both parallel and nonparallel fracture walls [*Oron and Berkowitz*, 1998]. Yet, if the

flowing fluid is non-Newtonian, γ in equation (1) may significantly deviate from 3 [*Bird et al.*, 1987].

[8] In accordance with equation (1), the flow rate through the nth joint is given by

$$q_n = \int_{-c}^{c} dq_n = -\frac{2^{1-\gamma} W_*^{3-\gamma}}{3\eta} \frac{\partial p}{\partial z} \int_{-c}^{c} [W_n(x)]^\gamma dx, \qquad (2)$$

where c is the joint half-size (Figure 2a) and $W_n(x)$ is the aperture of the nth joint. Then the total flow rate through the set of N joints can be written as

$$q = \sum_{n=1}^{N} q_n = -\frac{2^{1-\gamma} W_*^{3-\gamma}}{3\eta} \frac{\partial p}{\partial z} \sum_{n=1}^{N} \int_{-c}^{c} [W_n(x)]^\gamma dx. \qquad (3)$$

[9] Comparing equation (3) to the Darcy law

$$\frac{q}{2cL} = -\frac{k}{\eta} \frac{\partial p}{\partial z}, \qquad (4)$$

the (effective) permeability, k, of a set of N joints can be expressed as

$$k = \frac{2^{-\gamma} W_*^{3-\gamma}}{3cb(N-1)} \sum_{n=1}^{N} \int_{-c}^{c} [W_n(x)]^\gamma dx, \qquad (5)$$

where $2cL$ is the cross-sectional area and $L = b(N-1)$ is the size of the joint set (Figure 2a).

[10] In particular, if the interaction between the joints is not taken into account, they all have an identical elliptical shape, $W_n^0(x) \equiv W_0(x) = 4p[(1-\nu^2)/E](c^2 - x^2)^{1/2}$ [e.g., *Tada et al.*, 1985], and expressions (3) and (5) result in

$$\begin{cases} q_0 = \dfrac{2^{1-\gamma} W_*^{3-\gamma} N}{3\eta} \left(-\dfrac{\partial p}{\partial z}\right) \displaystyle\int_{-c}^{c} [W_0(x)]^\gamma \, dx \\ \quad = \dfrac{2^{1-\gamma} c W_*^3 N}{3\eta} \left(\dfrac{W_0}{W_*}\right)^\gamma \dfrac{\Gamma(1/2)\Gamma(1+\gamma/2)}{\Gamma[1+(\gamma+1)/2]} \left(-\dfrac{\partial p}{\partial z}\right) \\ k_0 = \dfrac{2^{-\gamma} W_*^{3-\gamma} N}{3cb(N-1)} \displaystyle\int_{-c}^{c} [W_0(x)]^\gamma \, dx \\ \quad = \dfrac{2^{-\gamma} W_*^3}{3b} \dfrac{N}{N-1} \left(\dfrac{W_0}{W_*}\right)^\gamma \dfrac{\Gamma(1/2)\Gamma(1+\gamma/2)}{\Gamma[1+(\gamma+1)/2]}, \end{cases} \qquad (6)$$

where here and further index "0" corresponds to the case of no interaction, $W_0 \equiv W_0(0) = 4pc(1-\nu^2)/E$, and the absence of the argument means that the corresponding aperture (W_0 in this case) is computed at the joint center, $x = 0$. In equation (6), $\Gamma(z)$ is the Gamma function and to derive equation (6), we used expressions (3.249.5) and (8.384.1) from *Gradshteyn and Ryzhik* [2000].

[11] Taking into account that $\Gamma(z+1) = z\,\Gamma(z)$, $\Gamma(1/2) = \sqrt{\pi}$, and $\Gamma(1) = 1$ [e.g., *Gradshteyn and Ryzhik*, 2000], in the case of Newtonian fluid, we have

$$\frac{\Gamma(1/2)\Gamma(1+\gamma/2)}{\Gamma[1+(\gamma+1)/2]} = \frac{3\pi}{8} \quad (\gamma = 3). \qquad (7)$$

[12] To evaluate the effect of joint elastic interaction, we first compare the permeabilities of the same joint set loaded by the same fluid pressure with and without accounting for joint interaction. Accordingly, we introduce the ratio of these permeabilities

$$\kappa = \frac{k}{k_0}, \qquad (8)$$

where k and k_0 are defined by equations (5) and (6) resulting in

$$\kappa = \frac{\Gamma[1+(\gamma+1)/2]}{\Gamma(1/2)\Gamma(1+\gamma/2)} \frac{1}{Nc} \sum_{n=1}^{N} \int_{-c}^{c} \left[\frac{W_n(x)}{W_0}\right]^\gamma dx. \qquad (9)$$

Note again that κ compares permeability of a joint set not to the stress-independent permeability, but rather to the case of stress-dependent permeability evaluated by ignoring the joint interaction.

[13] According to equation (9), to calculate κ, we shall compute the joint apertures, $W_n(x)$, in every point, x, along the joint axes (i.e., x axes in Figure 2b). As mentioned above, if the interaction between the joints is not taken into account, they all have an identical elliptical shape, $W_0(x)$, which, obviously, becomes different as a result of the interaction [e.g., *Germanovich and Astakhov*, 2004] and affects the fluid flow through the joints (see the next section).

[14] Because the fluid viscosity and pressure gradient are equal in both cases, the Darcy law (4) suggests that the permeability ratio can also be written as

$$\kappa = \frac{q}{q_0}, \qquad (10)$$

where the fluid flow rate, q_0, in the case of noninteracting joints is given by equation (6). Therefore, although we referred to κ as the permeability ratio, it can also be called the flow rate ratio or, shorter, flow ratio, which also characterizes the effect of joint interaction on the fluid flow rate through a given set of joints. Furthermore, the "permeability ratio" only refers to the ratio of effective permeabilities. According to the definition of the effective permeability, the flow rates through the joint set and through the equivalent continous medium with effective permeability are equal. Hence, in essence, the permeability ratio simply represents the flow ratio.

[15] In the case of non-Newtonian fluids, it may be unclear how to define permeability while the concept of flow ratio (10) still can be used as a convenient way to characterize the effect of joint interaction. Consider, for example, the "power law" non-Newtonian fluid, which is characteristic for many petroleum liquids [e.g., *Gidley et al.*, 1989; *Economides and Nolte*, 2000]. In this case, the viscosity, η, in the constitutive relation $\tau_{yz} = -\eta dv_z/dy$ exhibits the power law relation $\eta = \eta_0 |dv_z/dy|^{m-1}$, where m and η_0 are the exponent and consistency index in the power law model, respectively, τ_{yz} is the shear stress in the fluid, and v_z is the velocity of the fluid flow along the joint (in the coordinate set shown in Figure 2b). For the symmetrical steady state flow (Figure 2b), the motion equation, $\partial\tau_{yz}/\partial y +$

$\partial p/\partial z = 0$, suggests that $\tau_{yz} = -y\partial p/\partial z$ and, therefore, $-\eta_0|dv_z/dy|^{m-1}(dv_z/dy) = -y\partial p/\partial z$. Hence $|dv_z/dy| = |y(\partial p/\partial z)/\eta_0|^{1/m}$, so that the fluid viscosity, $\eta = \eta_0^{1/m}|y\partial p/\partial z|^{1-1/m}$, depends upon the position, y, across the fluid flow. This observation does not allow the use of constant viscosity in the Darcy law (4). Accordingly, defining the effective permeability, k, becomes rather ambiguous (unless some sort of effective viscosity is introduced as well, which is not a unique procedure).

[16] Yet employing the flow ratio (10) is quite straightforward when instead of using equation (1), a slightly more complex but essentially similar expression [e.g., see *Bird et al.*, 1987]

$$dq = \frac{2}{(2+1/m)\eta_0^{1/m}}\left(\frac{W}{2}\right)^{2+1/m}\left(-\frac{\partial p}{\partial z}\right)^{1/m}dx \qquad (11)$$

is employed. Substituting equations (11) into (10) and taking into account that the fluid parameters, m and η_0, are the same for interacting and noninteracting joints, we have

$$\kappa = \frac{q}{q_0} = \frac{\sum_{n=1}^{N}\int_{-c}^{c}[W_n(x)]^{2+1/m}dx}{N\int_{-c}^{c}[W_0(x)]^{2+1/m}dx}, \qquad (12)$$

which, considering equation (6), becomes identical to equation (9) if we chose $\gamma = 2 + 1/m$.

[17] Note that the effective hydraulic conductivity, $K = k\rho g/\eta$, where ρ is the fluid density and g is the gravitational acceleration, could also be used instead of effective permeability, k. Obviously, in the case of the incompressible fluid, as considered here, $K/K_0 = q/q_0$, such that κ can also be called the "ratio of hydraulic conductivities."

[18] Because the joint apertures, $W_n(x)$, in equation (3) are functions of (internal) fluid pressure and (remote) confining stresses as well as elastic properties, as follows from equations (3), (5), and (6), stress-dependent permeability and fluid flow rate do depend upon these parameters. In contrast, the flow/permeability ratio, κ, is strictly a geometrical parameter of flow network structure (even in the case of non-Newtonian, power law fluids) because the fluid pressure, confining stress, and elastic properties are the same for both q and q_0, so that they cancel each other in equation (12) (see also equation (9)). Accordingly, in the case of parallel joints, κ is the function of only two geometrical parameters, that is, $\kappa = \kappa(s, N)$.

[19] As an example, consider *Nolte*'s [1987] model that accounts for the interaction of $N \geq 2$ closely spaced, identical parallel fractures. In this and similar models [e.g., *Ben Naceur and Roegiers*, 1990], all the joints are assumed to be equally opened and the total (combined) aperture of N joints is the same as the aperture of one isolated joint of the same size, $2c$. In other words, $W_n(x) \approx (1/N)W_0(x)$ ($N \geq n \geq 1$, $N \geq 1$). This assumption has significantly impacted the understanding of multisegmented hydraulic fractures in petroleum production (see reviews in the work of *Mahrer et al.* [1996], *Germanovich et al.* [1998]) and supposedly is asymptotically accurate in the case of small spacing [e.g., *Ben Naceur and Roegiers*, 1990]. Then the flow rate, q, and permeability, k, of the set of N joints are easily obtained by replacing $W_n(x)$ in equations (3) and (5) with $W_0(x)/N$ and comparing the obtained results with equation (6):

$$k = \frac{k_0}{N^\gamma} \qquad q = \frac{q_0}{N^\gamma}. \qquad (13)$$

[20] Below we show that this result, which is obviously equivalent to $\kappa = 1/N^\gamma$, strongly overestimates the effect of joint interaction. In particular, according to equation (13), regardless of s, $k \to 0$ and $q \to 0$ as $N \to \infty$ because the aperture of each joint monotonically decreases with growing N. At the same time, for the infinite array of joints, which characterizes permeability and fluid flow more realistically for large N (see section 3), $k \neq 0$ and $q \neq 0$ because each joint has a nonzero aperture even for $N \to \infty$ (and fixed s). Furthermore, the end-members of the joint set are wider open than internal joints (e.g., see Figure 3). As $s \to 0$ (and fixed N), all the internal joints eventually become closed by the interaction [*Germanovich and Astakhov*, 2004] while the apertures of the end-members approach half the aperture of one isolated, noninteracting joint (see the next section). In other words, $W_1(x) = W_N(x) \to \frac{1}{2}W_0(x)$, $W_n(x) \to 0$ ($n = 2, 3, \ldots N-1$) as $s \to 0$ and an asymptotically correct result is then given by equation (13) with $N = 2$, i.e., $\kappa = 1/2^\gamma$ rather than $\kappa = 1/N^\gamma$. Therefore *Nolte*'s [1987] assumption indeed drastically underestimates permeability and fluid flow rate, which is the direct result of too strong interaction between the joints in the model based on *Nolte*'s [1987] assumption, that is, $W_n(x) = (1/N)W_0(x)$.

[21] Another example is given by considering joint interaction in the model of an infinite array. For a large number of joints, it is appealing to assume that each joint in the set of N joints has the same aperture, $W_\infty(x)$, as that in the infinite array with equal spacing, s, i.e., that $W_n(x) \approx W_\infty(x)$ ($N \geq n \geq 1$, $N \gg 1$). Replacing $W_n(x)$ in equations (3) and (5) with $W_\infty(x)$, we have

$$\begin{cases} \kappa_\infty = \dfrac{q}{q_0} = \dfrac{k}{k_0} \\ q(s,N) = Nq_\infty(s) = \dfrac{2^{1-\gamma}W_*^{3-\gamma}N}{3\eta}\left(-\dfrac{\partial p}{\partial z}\right)\displaystyle\int_{-c}^{c}[W_\infty(x)]^\gamma dx, \\ k(s,N) = k_\infty(s) = \dfrac{2^{-\gamma}W_*^{3-\gamma}N}{3cb(N-1)}\displaystyle\int_{-c}^{c}[W_\infty(x)]^\gamma dx \end{cases} \qquad (14)$$

[22] Where $7_\infty(s)$ is the flow rate through one joint in the infinite array that has effective permeability $K_\infty(s)$. While q and k in equation (14) depend upon N, κ_∞ does not because q_0 and k_0 have the same dependence on N as q and k, respectively (compare equations (6) and (14)). Thus κ_∞ is independent of the number of joints. In particular, for an infinite array, $N \to \infty$ and the corresponding k_0 and k are easily obtained from equations (6) and (14) or directly from equations (4)–(6) by using $L = N\,b$ rather than $L = (N-1)b$. Below, it is convenient to use notation k_∞ in the case of an infinite array, i.e., $k_\infty = k_\infty(s) = k(s, N)$ ($N \to \infty$).

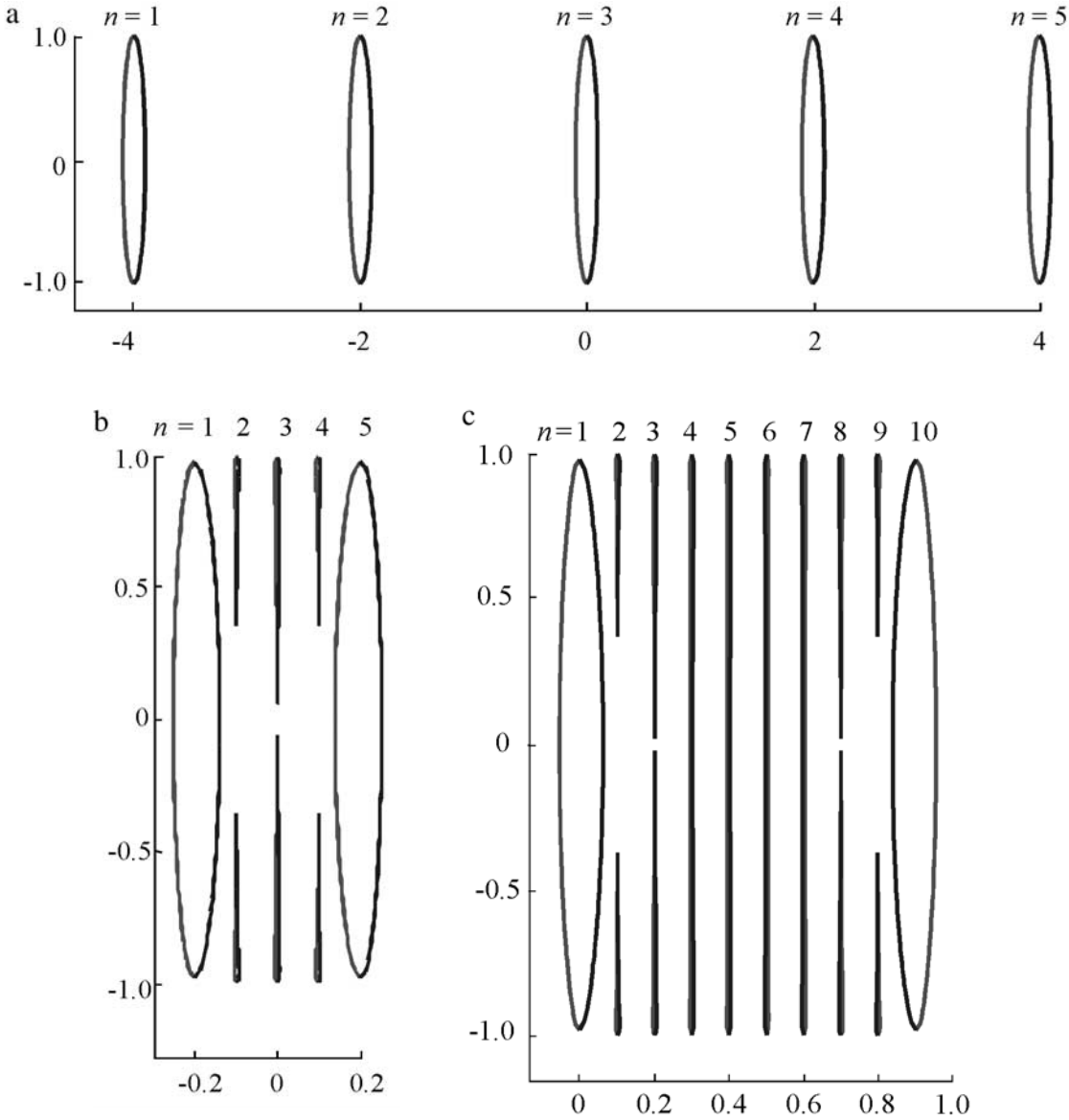

Figure 3. Apertures, normalized by $20cp/E_1$ (for better visualization), in the joint set with different number of segments, N, and spacing, s: (a) $N = 5$, $s = 1$; (b) $N = 5$, $s = 0.05$; (c) $N = 10$, $s = 0.05$; (d) $N = 10$, $s = 0.02$; and (e) $N = 20$, $s = 0.05$. All plots are shown in the normalized coordinates, x/c and y/c (Figure 2b). Closed parts of joints (with contacting sides) are not shown [see *Germanovich and Astakhov*, 2004].

[23] Since in the set of parallel joints, interaction suppresses openings of internal joints, clearly, k_0 provides an upper estimate of k. In the case of a non-Newtonian fluid, these permeabilities cannot be uniquely defined, but a similar argument applies to the fluid flow rates, q_0 and q. Furthermore, it appears that equation (14) represents a lower limit for κ, so that

$$\kappa_\infty < \kappa < 1, \tag{15}$$

and this fork cannot be improved since each bound represents a specific but asymptotically accurate case. Therefore further analysis is required to understand the intermediate cases. Such analysis is presented in the following sections where it is also shown that indeed κ_∞ represents a true lower bound.

[24] In the following sections, we use $m = 1$ (Newtonian fluid) and $\gamma = 3$ (cubic law) for all particular computations although it is obviously a trivial task to extend the obtained results to different m or γ.

3. Parametric Analysis

[25] To understand how interaction affects joint apertures and, consequently, permeability and flow rate, we performed the parametric analysis by varying s from 0.02 to 10 while N was changing from 1 to 50. We used the Boundary Collocation Method (BCM) based on Gauss-Chebysev integration as employed by *Germanovich and Astakhov* [2004] for computing both $W_n(x, N, s)$ and $W_\infty(x, s)$. Several examples are presented in Figure 3. The main computed quantities essential for this analysis are given in Tables 2 and 3.

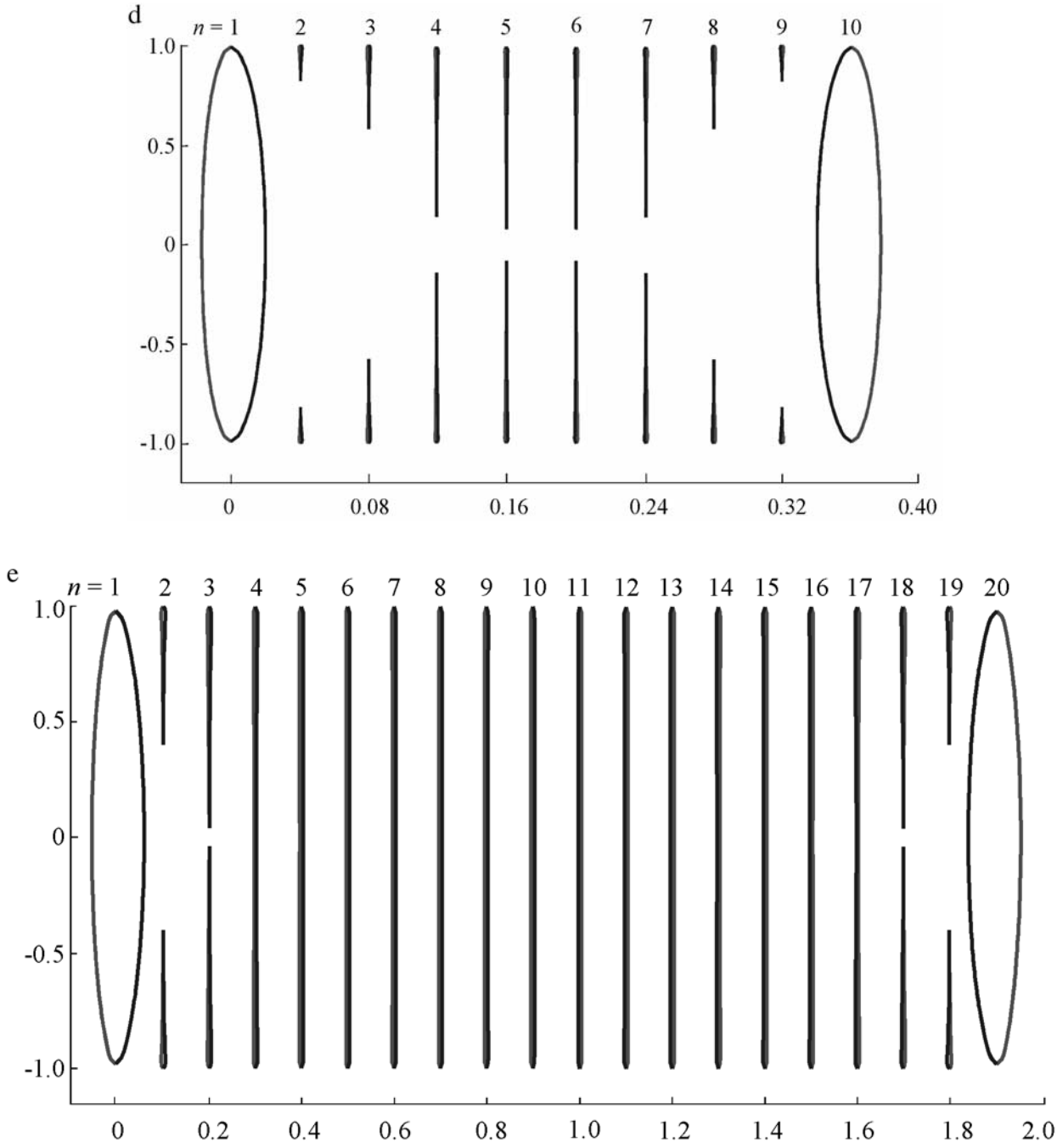

Figure 3. (continued)

[26] In the idealized joint setting shown in Figure 2a, two main parameters affect the joint apertures: (1) the number, N, of joints in the set and (2) the joint spacing, s. These parameters affect the apertures differently though. Reducing s results in *closure* of some internal joints (Figures 3a and 3b). Increasing N leads to reopening of these joints (Figure 3c). Further decrease of the spacing closes these joints again (Figure 3d).

[27] Since there is always a significant difference in the openings of edge and central joints, we present their apertures separately. Figure 4 shows ratios W_1/W_0 and W_1/W_∞, where W_1 is the aperture of the edge (end-member) joint (e.g., see Figure 3), W_0 is the aperture of a single (noninteracting) joint loaded by the same pressure, and W_∞ is the aperture of the joint in the infinite set (see Figure 3 for joint numbering convention and note that $W_1 = W_N$ due to the symmetry of the joint sets). Figure 5 presents similar ratios, W_c/W_0 and W_c/W_∞, for the central joint (e.g., joint 3 in Figures 3).

[28] Figure 4a shows the results for the ratio W_1/W_0. Since W_0 is the same for all curves, one can see that W_1, the aperture of the edge joint, differs little for various N. Nevertheless, it is peculiar to note that for $N > 3$, functions $W_1(s)$ have a local minimum and maximum before they approach the limit of $\frac{1}{2}W_0$ as $s \to 0$. In Figure 4a, this minimum is present for all $N > 3$ while the maximum is

Table 2. Computed Normalized Apertures, W_1/W_0, W_c/W_0, W_c/W_∞, and Flow/Permeability Ratios, κ, for Different Numbers, N, of Joints in the Set and Different Values, s, of Spacing[a]

N	s	10	5	3.33	2	1	0.5	0.33	0.2	0.1	0.05	0.02
2	W_1/W_0	0.996	0.986	0.969	0.923	0.799	0.659	0.605	0.563	0.531	0.515	0.506
	κ	0.989	0.957	0.910	0.790	0.526	0.312	0.243	0.191	0.156	0.140	0.131
3	W_1/W_0	0.995	0.982	0.962	0.909	0.777	0.646	0.604	0.583	0.565	0.532	0.512
	W_c/W_0	0.993	0.971	0.938	0.849	0.610	0.332	0.211	0.091	0	0	0
	W_c/W_∞	1.005	1.018	1.039	1.093	1.215	1.307	1.263	0.910	0	0	0
	κ	0.983	0.937	0.869	0.707	0.403	0.211	0.163	0.137	0.122	0.104	0.091
5	W_1/W_0	0.995	0.980	0.957	0.898	0.759	0.625	0.584	0.566	0.585	0.566	0.526
	W_c/W_0	0.991	0.964	0.924	0.821	0.572	0.320	0.224	0.144	0.069	0	0
	W_c/W_∞	1.003	1.010	1.023	1.057	1.139	1.260	1.341	1.440	1.380	0	0
	κ	0.978	0.916	0.829	0.632	0.305	0.132	0.094	0.076	0.078	0.072	0.060
7	W_1/W_0	0.994	0.979	0.955	0.894	0.751	0.616	0.573	0.555	0.576	0.595	0.540
	W_c/W_0	0.990	0.961	0.918	0.809	0.553	0.304	0.212	0.138	0.073	0.009	0
	W_c/W_∞	1.002	1.007	1.017	1.041	1.102	1.197	1.269	1.380	1.460	0.340	0
	κ	0.975	0.906	0.809	0.596	0.262	0.100	0.068	0.052	0.053	0.058	0.030
10	W_1/W_0	0.994	0.978	0.954	0.891	0.746	0.608	0.565	0.545	0.565	0.588	0.560
	W_c/W_0	0.989	0.959	0.914	0.800	0.539	0.291	0.201	0.130	0.072	0.036	0
	W_c/W_∞	1.001	1.005	1.012	1.030	1.074	1.146	1.204	1.300	1.440	1.440	0
	κ	0.972	0.897	0.792	0.566	0.228	0.077	0.049	0.036	0.035	0.038	0.035
20	W_1/W_0	0.994	0.977	0.952	0.888	0.739	0.598	0.553	0.530	0.546	0.567	
	W_c/W_0	0.989	0.956	0.908	0.788	0.521	0.274	0.186	0.118	0.065	0.036	
	W_c/W_∞	1.001	1.002	1.006	1.014	1.038	1.079	1.114	1.180	1.300	1.440	
	κ	0.969	0.885	0.769	0.526	0.187	0.050	0.027	0.018	0.016	0.018	
30	W_1/W_0	0.994	0.977	0.952	0.887	0.737	0.595	0.548	0.524	0.537	0.556	
	W_c/W_0	0.988	0.955	0.906	0.785	0.515	0.268	0.180	0.113	0.061	0.034	
	W_c/W_∞	1.000	1.001	1.003	1.010	1.026	1.055	1.078	1.130	1.220	1.360	
	κ	0.968	0.880	0.760	0.512	0.172	0.041	0.021	0.012	0.010	0.011	
50	W_1/W_0	0.994	0.978	0.951	0.886	0.735	0.592	0.544	0.518	0.529	0.544	
	W_c/W_0	0.988	0.955	0.904	0.782	0.510	0.262	0.176	0.108	0.057	0.031	
	W_c/W_∞	1.000	1.001	1.001	1.006	1.016	1.031	1.054	1.080	1.140	1.240	
	κ	0.966	0.867	0.752	0.498	0.159	0.034	0.015	0.008	0.006	0.010	
∞	W_∞/W_0	0.988	0.954	0.903	0.777	0.502	0.254	0.167	0.1	0.05	0.025	0.01
	κ	0.966	0.871	0.741	0.482	0.143	0.024	0.008	0.002	$3\cdot10^{-4}$	$3\cdot10^{-5}$	$1\cdot10^{-6}$

[a]Zero apertures refer to closed joints.

clearly seen for $N = 5$ and lies beyond the range of our calculations for $N = 10$, 20, and 50. Figure 4b shows the same ratio, W_1/W_0, as a function of the normalized distance, $L/(2c) = (N - 1)s$, between the edge joints, that is, as a function of the normalized joint set size (Figure 2a). It can clearly be seen that the curve for $N = 2$ envelops all other curves. This indicates that the values of all local maxima in Figure 4a, including those beyond the range of our calculations, are bounded by W_1/W_0 for the set of two joints that have the same size, $L/(2c) = (N - 1)s$. In this sense, the case of two joints represents the extreme of the largest joint aperture for a given joint set size. Furthermore, since all the maxima and minima in Figures 4a and 4b lie between the W_1/W_0 values of 0.5 and 0.6, this suggests that the deviations of $W_1(s, N)$ from the monotonic dependencies do not exceed 17%, which does not significantly affect joint set permeability.

[29] The curves of W_1/W_∞ in Figure 4c almost coincide because although now W_∞ depends upon s, it is still the same for all curves and the scale in Figure 4c is much greater than that in Figure 4a (the small differences between the curves in Figure 4c are practically not visible). Note that the total, combined aperture, $2W_1$, of the edge joints in a closely spaced joint set is roughly (exactly in the extreme case of $s \to 0$) the same as the aperture, W_0, of a single, noninteracting joint of equal size, $2c$. However, for sparsely spaced joints, $W_n = W_0$ (as $s \to \infty$) for any n, which significantly affects the corresponding flow rates and permeabilities (see below).

[30] Figure 5a illustrates that for $N \geq 10$, the aperture, W_c, of the central joint depends considerably upon the joint spacing, s, but only weakly on the number of joints, N. Figure 5b confirms the expectation that W_c should approach W_∞ as N increases (see also Figure 3e). However, Figure 5b

Table 3. Computed Joint Aperture Ratios, W_1/W_0, W_c/W_0, W_c/W_∞, and Flow/Permeability Ratios, κ, for Different Numbers of Joints, N, and the Corresponding Critical Values, s_{cr}, of Joint Spacing, s

N	3	4	5	7	10	20	30	50
s_{cr}	0.129	0.095	0.093	0.092	0.093	0.094	0.095	0.095
W_1/W_0	0.584	0.593	0.590	0.581	0.570	0.550	0.541	0.531
W_c/W_0	0	0	0.062	0.064	0.063	0.060	0.058	0.055
W_c/W_∞	0	0	1.319	1.391	1.340	1.277	1.208	1.146
κ	0.133	0.101	0.079	0.054	0.036	0.016	0.010	6.0×10^{-3}

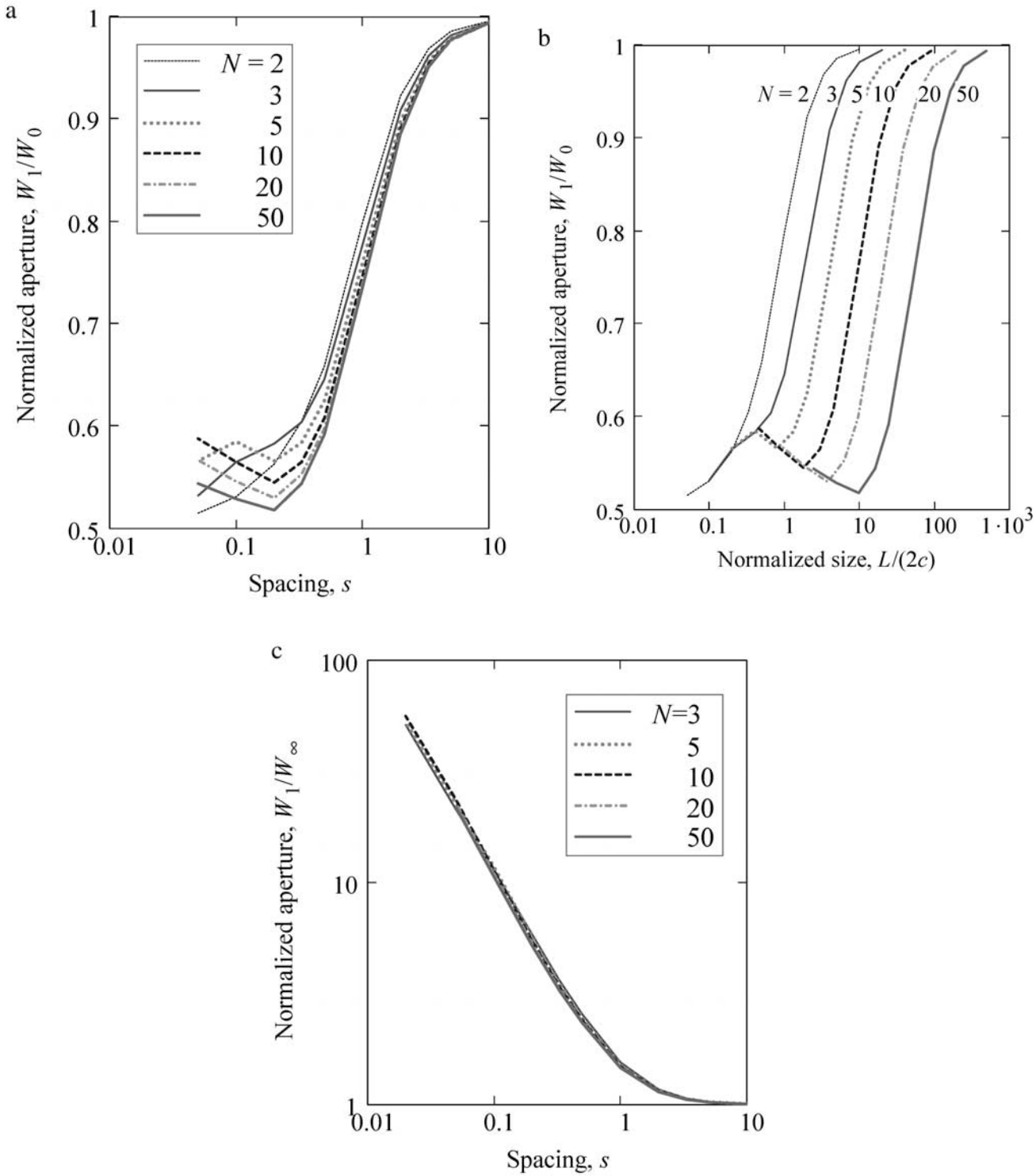

Figure 4. Normalized apertures (a and b) W_1/W_0 and (c) W_1/W_∞, as functions of spacing, s, for different numbers of joints, N, in the set (indicated in the legends). In Figure 4b, normalized size, $L/(2c)$, of the joint set (see also Figure 2a) equals $(N - 1)s$, i.e., normalized distance between two edge joints.

also shows that W_c approaches W_∞ slower for the smaller s. Therefore for closer joints, a greater number of joints in the set is required for the approximation of the infinite set to be sufficiently accurate for computing the apertures of the central joints.

[31] The discussion above shows that although it is often tempting to replace a set with $N \sim 10$ joints (more so for $N > 10$) by an infinite array (see equation (14)), this should be done with some care. For example, for $N = 10$ joints located rather sparsely at $s = 1$, the relative error, $\delta = (W_e - W_\infty)/W_c$, of this approximation is 6.9% while increasing N to 50 decreases this error to 1.6%. For $N = 10$ joints spaced more densely at $s = 0.1$, $\delta = 30.5\%$ while for $N = 50$ joints and the same $s = 0.1$, the error is $\delta = 12.3\%$. Note that these

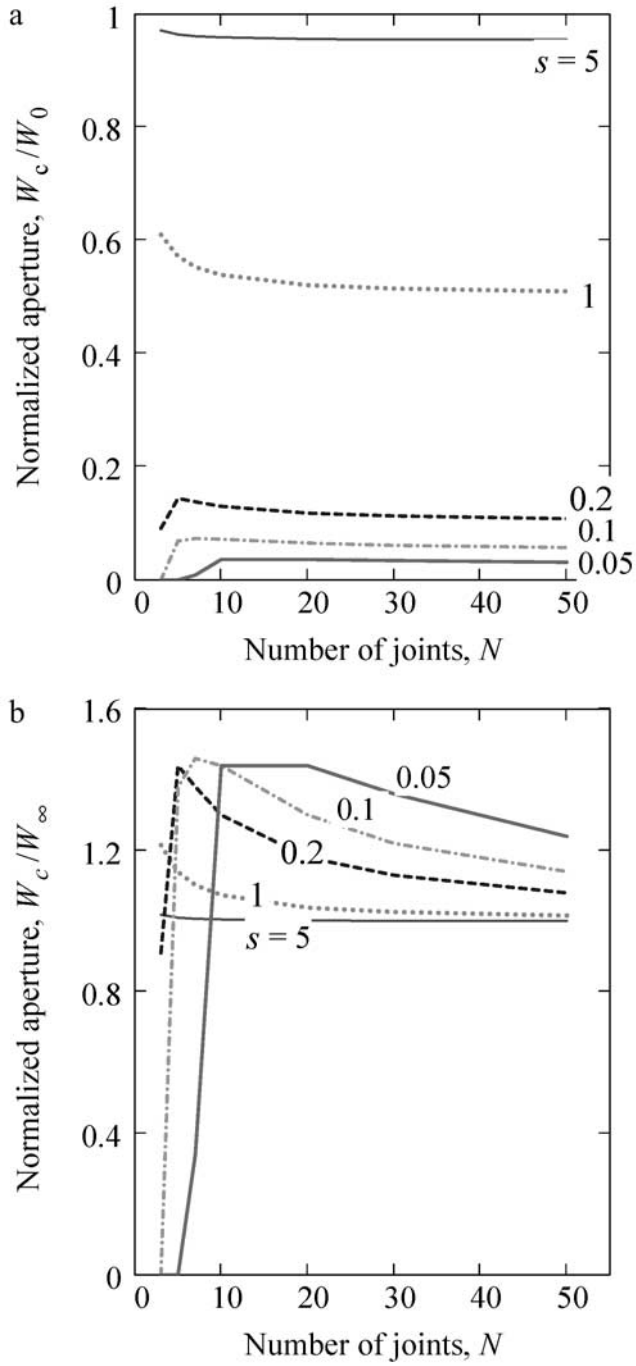

Figure 5. Normalized apertures (a) W_c/W_0 and (b) W_c/W_∞, as functions of the number of joints, N, in the set for different values of spacing, s (indicated in the legends).

errors were calculated with respect to the joint apertures while the corresponding flow rates and permeabilities can be affected more seriously (see below).

[32] Thus Figures 4 and 5 illustrate that the apertures of edge and internal joints in a closely spaced set differ considerably, which, in turn, may significantly affect the pattern of fluid flow. This can clearly be seen from Figure 6 that shows the fraction

$$f = \frac{q_1 + q_N}{\sum_{n=1}^{N} q_n} \tag{16}$$

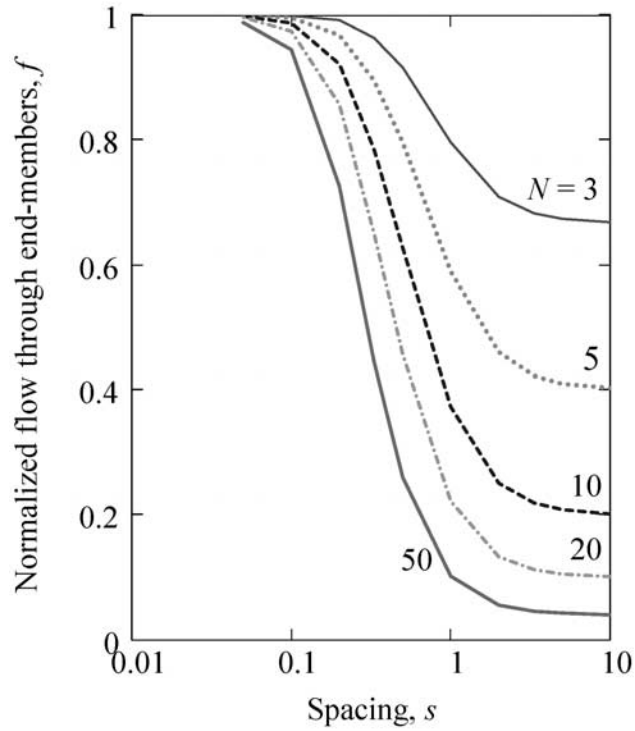

Figure 6. Normalized fluid flow (equation (16)) through the end-members as a function of joint spacing, s, for different numbers of joints, N, in the set (indicated in the legend). This ratio tends to zero for $N \to \infty$.

of the fluid flow, $q_1 + q_N$, through two edge joints with respect to the combined flow, q, through all joints as a function of joint spacing, s. One can see that for $s < 0.1$, only a small fraction of the fluid flows through internal

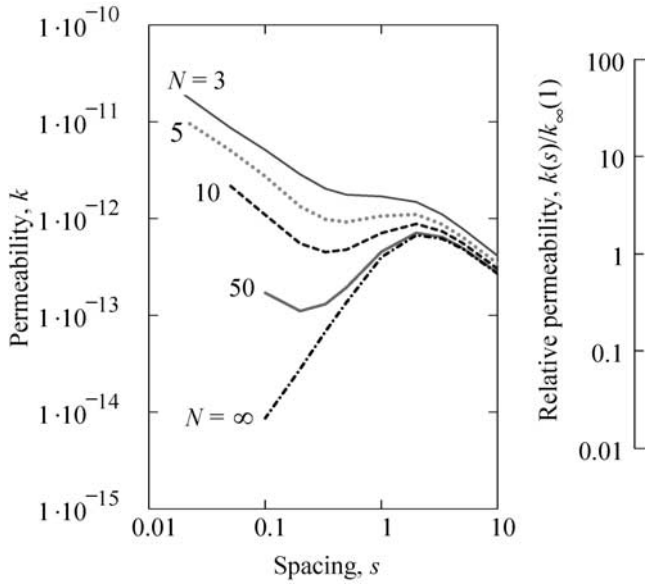

Figure 7. Permeability, k, of a set of joints as a function of joint spacing, s, for different numbers, N, of joints in the set (indicated in the legend). Left vertical scale shows k in m^2, while the right scale corresponds to the relative permeability, $k(s)/k_\infty(1)$.

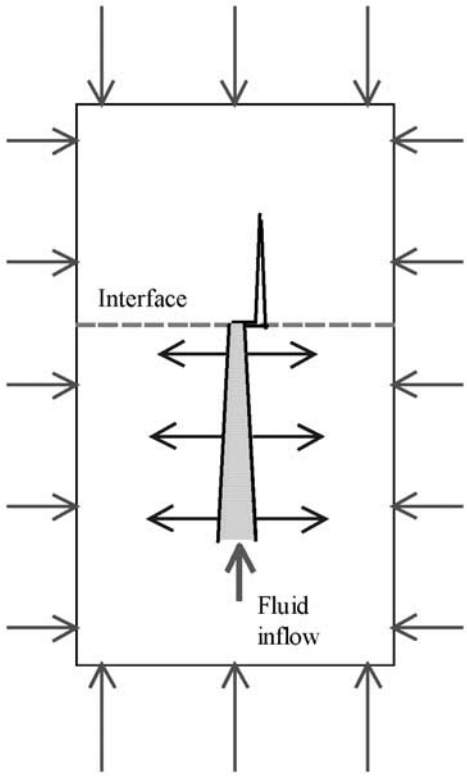

Figure 8. A mechanism of fracture confinement: if a pressurized fracture grows beyond an interface between two different rock layers and deviates from its plane [e.g., *Renshaw and Pollard*, 1995], the fluid inflow into the tip zone will be restricted by the ''turn'' (tortuosity), considerably reducing the pressure after the interface. Similar to *Barenblatt*'s [1962] process zone, the confining stress (shown by arrows) will then suppress further crack growth.

joints (within the considered range of N). For example, for $N = 50$ and $s = 0.1$, 94.5% of the total fluid flow passes through the two edge joints while only 5.5% of the fluid flows through the remaining 48 joints between them. This result suggests that indeed as a result of joint interaction, the fluid flow through the joint set may become highly nonuniform and focused at the set edges.

[33] The bulk permeability of jointed rock is also considerably affected by joint interaction. This can be observed from Figure 7, which shows the dependence of the overall permeability, k, of a joint set on the joint spacing, s. In plain strain elasticity, the crack opening displacement depends upon the elastic properties of the host material. However, the relative permeability, $k(s)/k_\infty(1)$, does not depend on those (right vertical scale in Figure 7). To estimate the expected permeability changes in a typical formation ($E = 10^{10}$ Pa, $\nu = 0.25$), we also present in Figure 7 (left vertical scale) the absolute value, $k(s)$, of permeability computed directly from equation (5). Since permeability is linearly related to the excess pressure, p, applied inside the joints, any value of p can be chosen for a particular computation as long as joints do not propagate for the chosen value. As an extreme yet characteristic case, we chose for the value of p the largest normal traction at which one isolated joint is just about to propagate vertically. This value is determined from the condition, $K_I = K_{Ic}$, of fracture propagation, where K_I is the stress intensity factor [e.g., *Tada et al.*, 1985] at the fracture front (tip), and K_{Ic} is the fracture toughness of the host material. For most rocks the typical value of K_{Ic} is $\sim$1 MPa $\times$ m$^{1/2}$ [e.g., *Atkinson and Meredith*, 1987]. Since the stress intensity factors at the tips of all joints in a parallel set are smaller than K_I at the tip of the isolated (noninteracting) joint, it is expected that no joint in the set will propagate at this pressure ($p = 0.56$ MPa for joints of $2c = 1$ m size and $K_{Ic} = 1$ MPa $\times$ m$^{1/2}$). Note that even if $K_I > K_{Ic}$, this does not necessarily mean that joints will propagate vertically any considerable distance after they cross the bedding interfaces (Figure 8).

[34] Joint spacing, s, affects the set permeability, k, in two ways. On the one hand, decreasing s grossly results in the closure of the parallel joints (because of their interaction; see Figure 3 and Table 2). On the other hand, more joints appear in the unit area (normal to fluid flow direction) with decreasing s, resulting in the permeability increase (see equation (4)). As can be seen from Figure 7, for any N (including $N = \infty$), k increases with decreasing s until $s \approx 1.7$. For $s > 1.7$, joints in the set are located relatively far from each other so that the interaction is not yet strong enough to close them considerably, but this factor becomes more dominant with the increasing density of joints (i.e., with decreasing s). With a further decrease in spacing, i.e., for $s < 1.7$, the interaction significantly reduces the aperture of internal joints (Figure 5a) while it only weakly affects the edge joints (Figure 4a). Accordingly, k decreases until the contribution of the internal joints becomes negligible, focusing essentially the entire flow through the edge joints. This corresponds to the minima in Figure 7 because for smaller spacing (and fixed N), (a) internal joints are practically closed (e.g., see Figures 3 and 5) and do not contribute to the flow anymore, (b) the aperture of the edge joints does not change considerably (Figures 3 and 4a), and (c) the total area occupied by the joint set decreases. Note that the minimum and maximum do not appear for $N = 3$ since the contribution of only one central joint is not strong enough and most of the flow occurs through the edge joints even for large s. For greater N, however, the internal joints do contribute considerably to the fluid flow if the spacing is sufficiently large while the edge joints start dominating only at smaller s. This, in fact, is the main reason for the minima and maxima in Figure 7.

[35] As discussed above, it is appealing to introduce a permeability model based on the infinite array of parallel joints (see equation (14)). Figure 7 also shows the consequence of this limit ($N \to \infty$). Since there are no edges (end-members) in the infinite set, the corresponding permeability, k_∞, decreases monotonically with decreasing spacing. One can see that the absolute value of k_∞ can be orders of magnitude smaller than k for the corresponding set with finite number of joints. Furthermore, k_∞ decreases while for closely spaced joints, k increases with decreasing s.

[36] Finally, Figure 9 presents the results of the calculations of the flow ratio, $\kappa = q/q_0 = k/k_0$, which allows the comparison of the stress-dependent flow rates/permeabilities for interacting and noninteracting joints. One can see

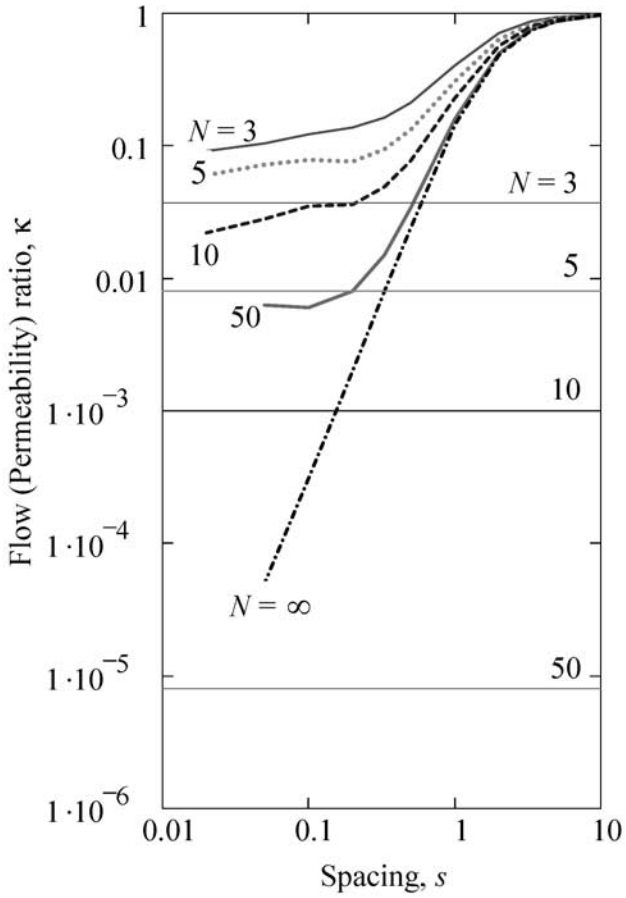

Figure 9. Permeability/flow ratio, κ, as a function of joint spacing, s, for different numbers, N, of joints in the set (indicated on the plots). Curves represent results of this work (based on equations (6), (7), and (9)) while horizontal straight lines correspond to *Nolte*'s [1987] approximation given by expression (13).

from Figure 9 that, as expected, $\kappa \approx 1$ for large spacing ($s \gg 1$). In this case, joint interaction does not result in q and k significantly differing from q_0 and k_0, respectively, i.e., $q \approx q_0$ and $k \approx k_0$. For $s \sim 1$ and smaller, generally, $\kappa \ll 1$ (i.e., $q \ll q_0$ and $k \ll k_0$). Accordingly, as can be seen from Figure 9, the stress-dependent permeability, k_0, and flow rate, q_0, determined without taking into account the joint interaction, can be one or two orders of magnitude greater than the accurate result because most of the joints in the set suppress each other as a result of their interaction.

[37] Figure 9 also suggests that if the interaction between the joints is taken into account based on the model of an infinite array of equally spaced joints (see equation (14)), the resulting flow/permeability ratio can be significantly underestimated. For example, for $s = 0.1$, replacing the set with $N = 50$ joints by the corresponding infinite array results in κ, which is an order of magnitude lower than that computed accurately. Furthermore, considering $N = 10$ joints as an infinite array (which is in concert with conventional wisdom) leads to an error of more than two orders of magnitude (see Figure 9). Note that not accounting for the interaction will result in the permeability overestimate (see inequalities (15)).

4. Asymptotic Approximation

[38] The above consideration leads to the following conclusions on the asymptotic behavior of the flow ratio, κ, as a function of the joint set parameters, that is, the number of joints, N, and the joint spacing, s. The rather obvious upper limit, κ_{max}, of κ is given by the case of noninteracting joints, which have the widest possible aperture, W_0, for a given pressure and joint size. Then κ_{max} is a function of s alone (see equation (6)), $\kappa_{max} = 1$ as $s \to \infty$, and this limit cannot be improved. The *lower* limit, κ_{min}, is less apparent since it is a function of both N and s. However, for any finite N, the aperture, $W_1 = W_N$, of the edge segments, approaches $\frac{1}{2}W_0$ while the apertures, W_n ($n = 2, \ldots, N-1$), of internal joints tend to zero as s decreases (see Figure 3 and Table 2). These two extremes result in the limiting value

$$\kappa_{min} = \frac{q_{min}}{q_0} = \frac{k_{min}}{k_0} = \frac{1}{q_0}\sum_{n=1}^{N} q_n = \frac{1}{4N} \qquad (s \to 0,\ N = \text{const}) \tag{17}$$

since $q_1 = q_N \to q_0/(8N)$ and $q_n \to 0$ ($n = 2, \ldots, N-1$) if $s \to 0$.

[39] On the other hand, for $N \to \infty$ and any fixed s, the apertures, W_c, of the central joints approach those of joints in the infinite set, i.e., W_∞. For sufficiently large N (which depends on s), the number of such central joints becomes great enough for the contribution of the set edges to be negligible (e.g., see Figure 6). In this extreme of $N = \infty$, κ is a function, $\kappa_\infty(s)$, of s only. At present, function $\kappa_\infty(s)$ can only be obtained by numerically computing $W_\infty(x)$ numerically [see *Germanovich and Astakhov*, 2004] and using equation (14). Nevertheless, two asymptotes, as $s \to \infty$ and $s \to 0$, are available. The first one corresponds to the case of noninteracting joints and represents the upper limit, $\kappa_{max} = 1$, of κ, which means that $\kappa_\infty(s) \to 1$ as $s \to \infty$. The second one corresponds to the case of infinitesimally close joints, so that the pressure, p, applied to the joint sides homogeneously compresses the ideally thin slab between the joints (Figure 10a). Then, except for the small proximities of the joint tips, the joint sides are displaced almost uniformly and become practically parallel (Figure 10a) [see also *Germanovich and Astakhov*, 2004, Figure C2]. Therefore, for small s, $W_\infty(s)$ is proportional to s in the leading term. Consequently, $\kappa_\infty(s) \propto s^3$ when $s \to 0$ because for small s, $W_\infty(x)$ is almost constant along the joints while $W_0(x)$ does not depend upon s (see also equation (6)).

[40] Therefore $\kappa_\infty(s)$ can now be approximated by

$$\kappa_\infty(s) = \frac{s^3}{s^3 + as + b}, \tag{18}$$

which has correct asymptotics for both small and large s and any values of parameters a and b. We chose these parameters by fitting equation (18) to the data for the ratio κ presented in Table 2. The least square method gives the values of $a = 3.546$ and $b = 2.931$, showing very good agreement between the computed and approximated results (Figure 11).

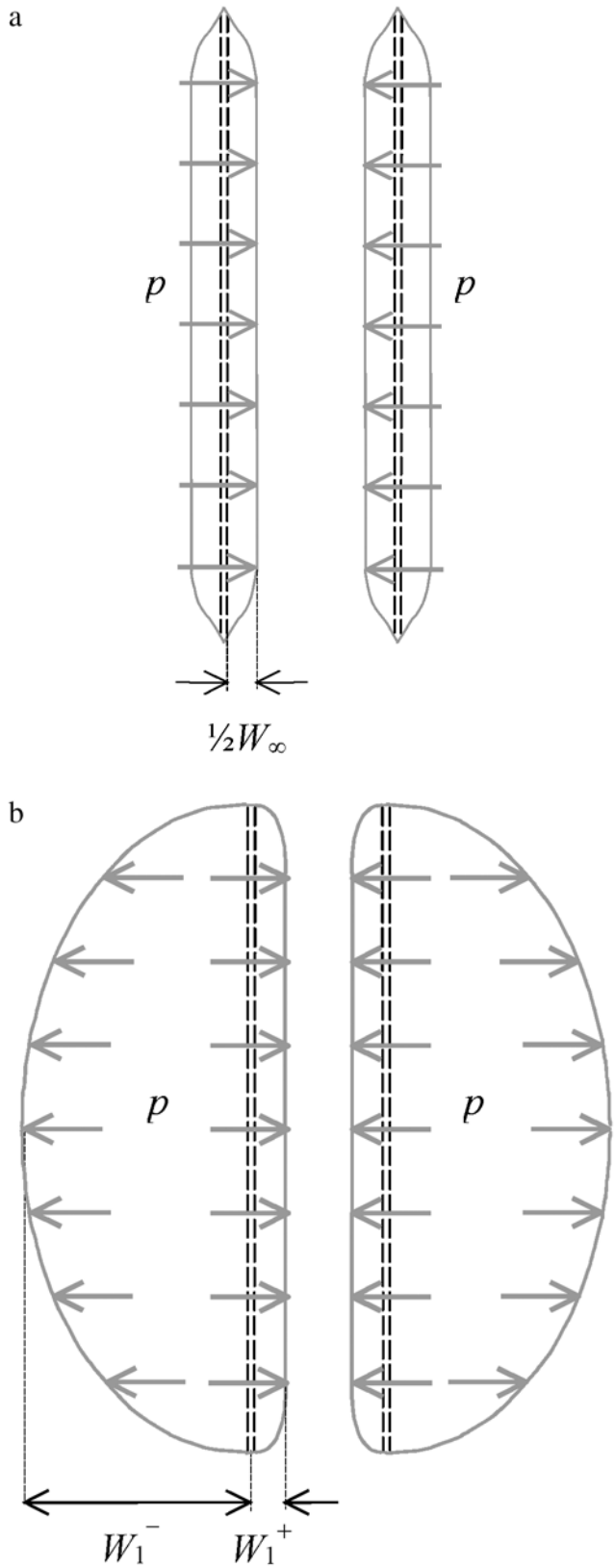

Figure 10. Leading asymptotic components of the joint side displacements in (a) the infinite array (only two neighboring joints are shown) and (b) a set of two joints. Dashed lines indicate the original positions of the joint sides while solid curves show the deformed state. See color version of this figure in the HTML.

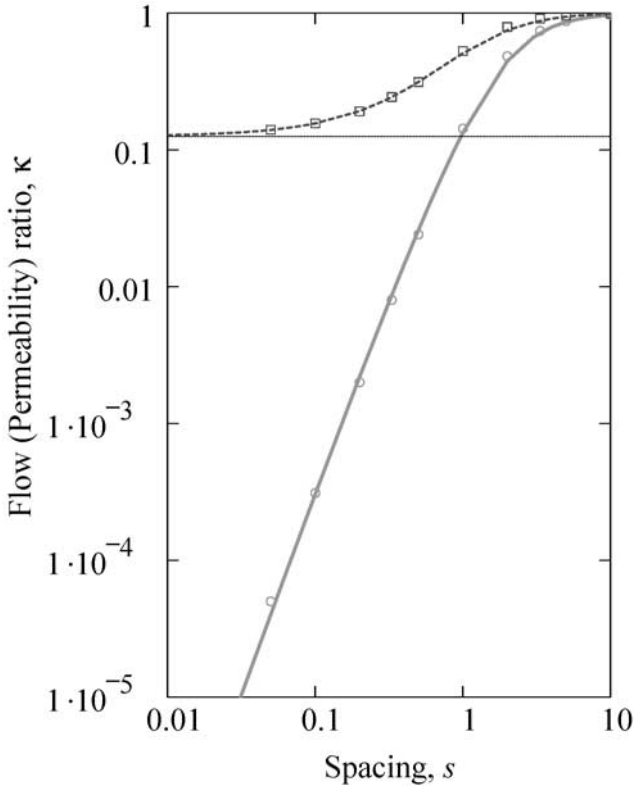

Figure 11. Comparison of the closed-form approximations (lines) with computed results for functions $\kappa_\infty(s)$ (circles) and $\kappa_2(s)$ (boxes) given by expressions (18) and (19), respectively (see also Table 4). See color version of this figure in the HTML.

[41] Another extreme, which can be considered as an opposite to the case of $N \to \infty$, is given by the set with $N = 2$ joints ($N = 1$ represents a trivial case). Similarly to the infinite array, κ is a function, $\kappa_2(s)$, of s alone and for arbitrary s, this function can only be obtained numerically. Yet, two asymptotes, for $s \to \infty$ and $s \to 0$, are also available in this case, so that $\kappa_2(s) \to \kappa_{max} = 1$ as $s \to \infty$ and $\kappa_2(s) \to \kappa_{min} = 1/8$ as $s \to 0$ (see equation (17)). These define the behavior of $\kappa_2(s)$ for the large and small s, respectively. The latter limit can be determined more accurately, however, by taking into account that the leading term of $W_1(x)$ for $s \to 0$ is given by $W_1^-(x)$, which corresponds to the displacement, $\frac{1}{2}W_0$, of the external joint sides (Figure 10b). Then the next term, $W_1^+(x)$, corresponding to the displacement of the internal joint sides (Figure 10b), is given by the compression of the ideally thin slab between the joints (see Figure 10b) by the homogeneous pressure, p, applied to the joint sides. Similar to the discussed above case of $N = \infty$ and small s, this additional term $W_1^+(x) \propto s$ (compare Figures 10a and 10b). Since $W_1^-(x) = O(1)$, $W_1^+(x)$ is of higher order and will be further omitted.

[42] Therefore a simple approximation given by

$$\kappa_2(s) = 1 - \frac{1}{cs^2 + ds + 8/7}, \tag{19}$$

also has correct asymptotics for both small and large s and any values of parameters c and d. In equation (19), the 8/7 term assures that $\kappa_2(s)$ has the correct limit, 1/8, for $s \to 0$, which corresponds to the leading term, $\frac{1}{2}W_0(x)$, in $W_1(x)$. The values of $c = 0.525$ and $d = 0.365$, also obtained by the least squares method, provide good agreement between the calculated and approximated results (Figure 11).

[43] All limiting cases for $\kappa(s, N)$ are summarized in Table 4. A simple interpolation between these cases is given by

$$\kappa(s, N) = \frac{4\kappa_\infty(s)(N-2) + 8\kappa_2(s)}{4N}, \tag{20}$$

which can be verified directly by comparing equation (20) with Table 4. Note that approximations (18) and (19) are certainly not unique and can be replaced in equation (20) by any other appropriate functions as can be equation (20) itself. However, expressions (18), (19), and (20) have, probably, the simplest yet asymptotically correct forms and were chosen based on this consideration. This resulted in a sufficiently good agreement between the computed and approximated results (Figure 12) in the whole range of s and N. Indeed, the relative error given by equation (20) does not exceed 27%, which can be often ignored in most applications involving rock permeability. Such a relatively small inaccuracy is well compensated by the opportunity to evaluate the stress-dependent flow rate in joint systems with a very large number of joints. At present, $N \sim 10^2$ and $s \sim 10^{-2}$ represent the limits of the computations that can generally be conducted with the commonly available computer power. Though these parameters are within the range observed in the field (see, e.g., the review in the paper by *Germanovich and Astakhov* [2004]), they still could be far from what is needed from a practical standpoint, e.g., required for modeling large petroleum reservoirs [e.g., *Long et al.*, 1996]. The application of the closed-form formula (20) allows the estimation of the permeability/flow ratio, κ, for an arbitrarily large number of closely spaced joints. In fact, the greater N and the smaller s, the more accurate the results given by expression (20), while the case of very large N and small s is the computationally most difficult. An example for $N = 1000$ is shown in Figure 12 by the dashed curve, which would be a rather challenging task to compute numerically.

5. Discussion

[44] The adopted assumptions of constant spacing and equal joint size are not critical for the results obtained in the previous sections. Figure 13 demonstrates that regardless of details of joint spacing and layer thickness distributions, the fluid flow through the joint set may become highly heterogeneous and focusing in the end-members. This conclusion is rather robust and appears to be justified in the case of

Table 4. Asymptotic Properties of the Flow/Permeability Ratio, κ

Conditions	Limits	Auxiliary Limits
$s \to \infty$, N = const	$\kappa \to 1$	N/a[a]
$s \to 0$, N = const	$\kappa \to \frac{1}{4N}$	N/a
$N \to \infty$, s = const	$\kappa \to \kappa_\infty(s)$	$\kappa_\infty(s) \to 0$ ($s \to 0$)
		$\kappa_\infty(s) \to 1$ ($s \to \infty$)
$N \to 2$, s = const	$\kappa \to \kappa_2(s)$	$\kappa_2(s) \to 1/8$ ($s \to 0$)
		$\kappa_2(s) \to 1$ ($s \to \infty$)

[a]N/a, not applicable.

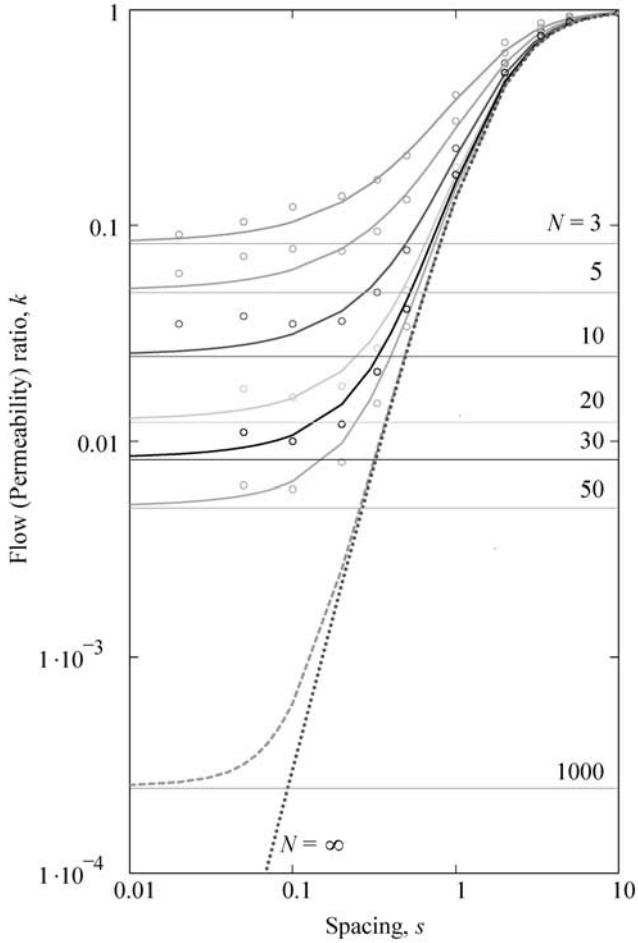

Figure 12. Comparison of the closed-form approximations (lines) with computed results (circles) for function $\kappa(s, N)$ given by expression (20). Horizontal lines show the limiting values, $1/(4N)$ ($\kappa(s, N) = 1/(4N)$ as $s \to 0$), for each N. Asymptotic approximations of $\kappa(s, 1000)$ and $\kappa_\infty(s) = \kappa(s, \infty)$ are shown by the dashed and dotted curves, respectively. See color version of this figure in the HTML.

uneven distances between the joints as long as the joint spacing is relatively close to critical $s_{cr} = 0.94$ (Table 3) [see also *Germanovich and Astakhov*, 2004]. In this case, the end-members (i.e., edge joints) will be widely opened while all internal segments will be suppressed by the interaction (as shown in Figures 3b–3e and 13). Nevertheless, it should be mentioned that for joint sets observed in the field, it is often difficult to determine the exact locations of the edges of the joint set (e.g., see Figure 1). As a zero approximation, the "edges" could be defined as places in the joint set where the spacing between the joints is of the order of the joint size (i.e., the lithological layer thickness) or greater. As Figure 3a suggests, the joint aperture should then not be notably affected by the interaction and, therefore, the neighboring joints separated by such a "large" distance will be widely open which corresponds to the edge conditions in the joint set.

[45] The existence of the maximum for $k(N, s)$ (Figure 7) was probably first suggested by *Bai and Pollard* [2001]. On the basis of the three-fracture model [*Bai et al.*, 2000], they computed the aperture, $W_c(x, N, s) = W_2(x, N, s)$ of the central fracture in the set of $N = 3$ fractures. They assumed that this fracture can be used to approximate the aperture, $W_n(x, N, s)$, of any fracture in a row composed of many ($N \gg 1$) equally spaced fractures. They further introduced the normalized volumetric flow rate, $\chi(s) = q(s)/q(1)$, where $q(s)$ and $q(1)$ are, respectively, the total flow rates in the fracture set with spacing s and in the reference fracture set of the same size, L, but with fracture spacing equal to the fracture size, i.e., $s = 1$.

[46] For the fracture set of size L (Figure 2a) and with spacing s, the number of fractures in the set is $N = 1 + L/b = 1 + L/(2cs)$ while for the reference set with $s = 1$, the number of fractures $N_1 = 1 + L/(2c)$. For a large number of fractures, $N = L/b = L/(2cs)$ and $N_1 = L/(2c)$ ($s = 1$), so that $N/N_1 = 1/s$. Since in the three-fracture model, $q_n(N, s)$ and $q_n(N, 1)$ are approximated by $q_2(3, s)$ and $q_2(3, 1)$, respectively, $q(s)$ and $q(1)$ can be represented by $Nq_2(3, s)$ and $N_1q_2(3, 1)$, where, as usual, $q_n(N, s)$ denotes the flow rate in the nth of N fractures. Therefore, according to the three-fracture model, χ can be approximated by $\chi_1 = (1/s)q_2(3, s)/q_2(3, 1)$.

[47] In the case of the infinite array, $q(s) = Nq_\infty(s)$ and $q(1) = N_1q_\infty(1)$ have a meaning of flow rates through the array segment of dimension L. We can then write $\chi = (1/s)q_\infty(s)/q_\infty(1)$, where $q_\infty(s)$ is the flow rate through one fracture in the infinite array. Apparently, such defined χ coincides with $k_\infty(s)/k_\infty(1)$ plotted in Figure 7 and we further compare the results obtained by the three-fracture method to the accurate computations based on equation (14) (see Appendix C in the paper by *Germanovich and Astakhov* [2004] for details on computing $W_\infty(s)$). Obviously, considering infinite array instead of the finite set of fractures does not change χ_1, that is, $\chi_1 = (1/s)q_2(3, s)/q_2(3, 1)$.

[48] Quantities χ and χ_1 are given in Table 5, which also includes the error, $\delta_1 = (\chi_1 - \chi)/\chi$ of approximating χ by χ_1, that is, computed based on the three-fracture model. Because χ and χ_1 are based on different normalization, these quantities do not converge with increasing spacing.

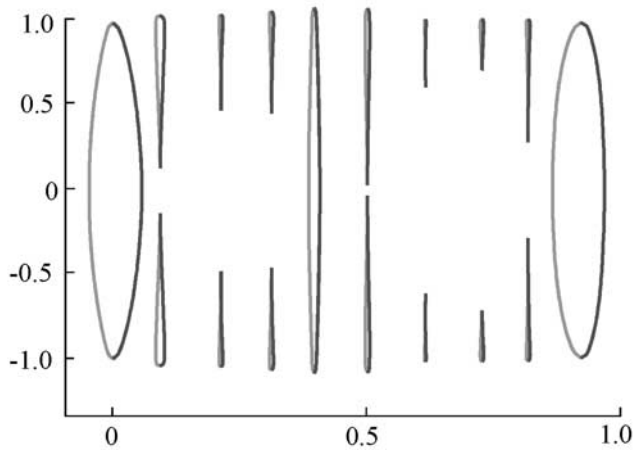

Figure 13. Apertures (normalized, for better visualization by $20c_mp/E_i$, where $2c_m$ is the mean joint size or layer thickness) in the joint set with $N = 10$ and slightly varying s and c (by 18.7% and 5.3% with respect to their mean values). In the calculations the mean normalized joint spacing $s_m = b_m/(2c_m)$ was 0.049, where b_m is the mean dimensional spacing. See color version of this figure in the HTML.

Table 5. Normalized Volumetric Flow Rates, χ, χ_1, and χ_2, and the Relative Errors, δ_1 and δ_2, Computed for Different Values of s

s	χ	χ_1	χ_2	δ_1,%	δ_2,%
5	1.27	0.746	1.282	−41.3	1.0
3.33	1.617	1.008	1.734	−37.4	7.3
2	1.733	1.255	2.158	−27.6	24.5
1	1	1	1.72	0	72.0
0.5	0.324	0.428	0.736	32.2	127.4
0.33	0.153	0.215	0.369	39.9	140.5
0.2	0.058	0.061	0.106	5.9	82.2
0.1	0.015	0.019	0.033	29.6	123.0
0.05	$3.82\cdot10^{-3}$	$4.86\cdot10^{-3}$	$8.36\cdot10^{-3}$	27.3	119.0
0.02	$6.17\cdot10^{-4}$	$9.47\cdot10^{-4}$	$1.63\cdot10^{-3}$	53.5	164.0

Indeed, if $s \to \infty$, $q_2(3, s) \to q_\infty(s)$, then $\chi_1 \to (q_\infty(1)/q_2(3, 1))\chi = 0.581\chi$, which corresponds to the limiting value of $\delta_1 = -42\%$ (compare to $\delta_1 = 41.3\%$ for $s = 5$ in Table 5). To clearer see how the three-fracture model represents the total fluid flow through the individual fractures in the fracture set, we also computed $\chi_2 = (1/s)q_2(3, s)/q_\infty(1) = (q_2(3, 1)/q_\infty(1))\chi_1 = 1.720\chi_1$. Comparing χ and χ_2 given in Table 5, we observe that although employing the three-fracture model overestimates the volumetric flow rate (i.e., $q_2(3, s) > q_\infty(s)$), the relative difference, $\delta_2 = (\chi_2 - \chi)/\chi$ between χ and χ_2 (i.e., between $q_\infty(s)$ and $q_2(3, s)$) reduces as s increases ($\delta_2 = 1\%$ for $s = 5$). This is of course expected since $W_2(x, 3, s) \to W_\infty(x, s) \to W_0(x)$ as $s \to \infty$. For sufficiently large s, the observed overestimation is due to the inequality $W_2(x, 3, s) > W_\infty(x, s)$, which can be explained by a greater (infinite) number of "neighbors" and, accordingly, larger constrain compared to the central fracture in the three-member set (that only has two "neighbors"). As s reduces, $W_2(0, 3, s)$ decreases faster than $W_\infty(0, s)$ (see also Table 2) and, in particular, the central fracture in the three fracture set closes at $s \le s_{cr}$ while $W_\infty(x, s) > 0$ for any s. However, the central fracture in the three-fracture sets still has open parts that are relatively weakly confined by "only" two and *relatively* more remote adjacent fractures. These open parts are still available for fluid flow, which in the three-fracture model is greater than that through the narrower though fully open fracture in the infinite array. Therefore, although somewhat counterintuitive, $\chi_1 > \chi$, or in other words, $q_2(3, s) > q_\infty(s)$, even in for small spacing, s. Note, that in the case of finite number of fractures, the three-fracture method disregards the (widest) end-members, so that χ_1 may underestimate χ.

[49] On the basis of the three-fracture model, *Bai and Pollard* [2001] obtained that the ratio χ_1 reaches its maximum value of 1.2 at $s \approx 1.7$. Accurately computed normalized volumetric flow ratio, χ, has a maximum value of 1.7 at $s \approx 1.7$ (see also Figure 7). Summarizing the above discussion, we note that similarly to the case of fracture aperture [*Germanovich and Astakhov*, 2004], the three-fracture model should be used with some care for evaluating the flow rate through a set of parallel fractures. More specifically, within the spacing range given in Table 5, the relative error resulting from employing this method can be ~50% for the total volumetric flow rate and ~150% for the volumetric flow rate through individual fractures, which may or may not be important depending upon the particular application.

[50] Taking into account the interaction based on *Nolte*'s [1987] suggestion of closely spaced and equally opened joints, that is, $W_n(x) \approx (1/N)W_0(x)$, results in formula (13), which, as discussed in section 2, considerably underestimates the permeability and flow rate. This can also be seen

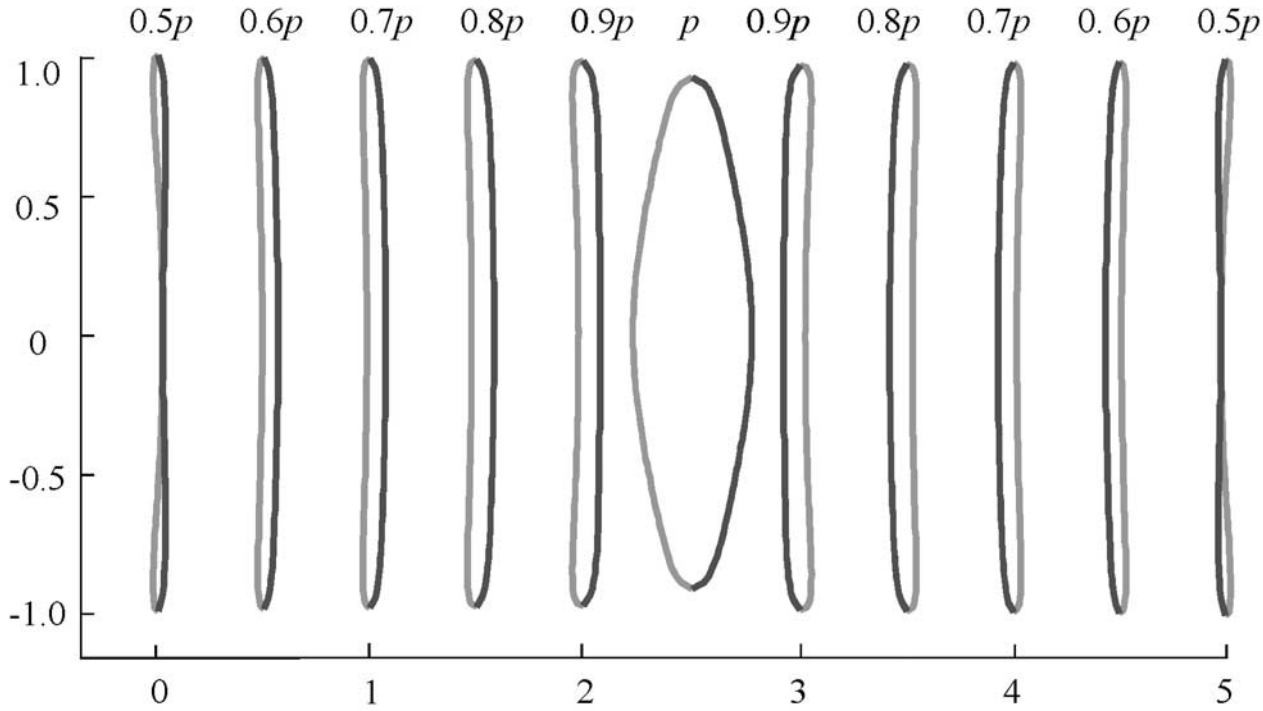

Figure 14. Apertures (normalized by $20cp/E_1$) of differently pressurized joints in the case of poor pressure communication between the joints. See color version of this figure in the HTML.

from Figure 9, where dependencies $1/N^3$, corresponding to equation (13), are shown by horizontal lines. Therefore *Nolte*'s [1987] approximation, while overestimating the interaction of joints, gives the lower bound for the permeability of the joint set in the case of small joint spacing. Note though that this bound is not very accurate since $\kappa \gg 1/N^3$ (Figure 9). For the case of large spacing, the approximation of an infinite array results in a more accurate lower boundary (see Figure 9). Apparently, the approximation of noninteracting joints gives the upper boundary for the permeability of a joint set.

[51] As was stressed in section 2, we assumed that the opening (net) pressure is equal in all joints. From a physical standpoint, this requires a good pressure communication between the joints, which, for example, can be provided by a secondary network of smaller fractures connecting the main joints. If the conductivities of the secondary fractures are not sufficiently large (e.g., if the secondary fractures are small), the pressure communication between the joints may be rather poor. In this scenario, joints will generally have different fluid pressures. Accordingly, joints with higher pressure could have larger apertures and most of the fluid would flow through them.

[52] Consider an example somewhat related to water injection into a fractured reservoir (C. Wright, personal communication, 2002). If pressure communication through the secondary fracture network is poor, the joint closest to the point of injection will have the maximum pressure. The pressure in other joints will generally decrease with increasing distance from the injection point. An example of linear pressure decrease is shown in Figure 14. In this case, the apertures of 11 joints, pressurized by the different pressures (indicated in Figure 14), increase from the end-members to the central part of the joint set and, therefore, most of the fluid flows through the central joints adjacent to the injection point (Figure 14). A rigorous analysis of this situation is beyond the scope of our paper but we can certainly conclude that the secondary fracture network may have a strong influence on the fluid flow distribution in the main fractures. Depending on the secondary permeability (in the direction perpendicular to the joints (i.e., *y*-direction in Figure 2b), the fluid flow can be highly heterogeneous, focusing in specific parts of the joint set. Note that as in the case of equal pressures in the joints, this effect is also a result of joint elastic interaction since otherwise the flow would be identical in all (noninteracting) joints.

6. Conclusions

[53] It is well known that the permeability of a set of joints can significantly vary in response to in situ stress conditions and pressure of the flowing fluid. Frequently, joint sets are closely spaced and although joint mechanical interaction could significantly affect their aperture, the interaction is usually ignored in the fluid flow models. It is rather obvious that this approach corresponds to the upper bound for flow rate and rock permeability. By taking into account the interaction between the joints, we show that modeling a joint set by an infinite array provides the lower bound. The difference between these bounds, however, can be rather large, so that they may not always be used with the sufficient accuracy.

[54] From the conceptual standpoint, it is often tempting to model a set with a finite number of joints by an infinite array. The results obtained in this work clearly demonstrate that such a model may result in a significant underestimation (by orders of magnitude) of both the permeability and flow rate. Similarly, the assumption of noninteracting joints may significantly overestimate (also by orders of magnitude) the stress-dependent permeability and flow rate compared to those computed more accurately when accounting for joint interaction.

[55] Because the internal pressure can, in fact, close the pressurized joints while two edge joints (end-members) in the set remain widely open (since they are not suppressed from one side by the adjacent joints), unless the number of joints in the set is exceedingly large (typically, $> 10^3$), the fluid flow through the joint set becomes highly heterogeneous, focusing in the edge joints. As a result, the permeability/flow rate dependence on the joint spacing is not monotonic, but has a maximum and a minimum. The derived closed-form expression for flow rate/permeability ratio is asymptotically accurate and allows computations for rather arbitrary joint sets.

[56] **Acknowledgments.** We thank the Associate Editor D. R. Schmitt and reviewer J. A. Hudson as well as the anonymous reviewer for their many helpful comments on an earlier version of this manuscript. The paper has considerably improved as a result of their diligent efforts. The authors are grateful to T. Bai, B. Berkowitz, B. J. Carter, A. Chudnovsky, F. Cornet, J. Desroches, E. Detournay, P. Dijk, V. Dunayevsky, A. V. Dyskin, A. R., Ingraffea, M. J. Mayerhofer, R. P. Lowell, E. Pasternak, D. D. Pollard, Z. Reches, L. M. Ring, J. Shlyapobersky, and M. D. Zoback for useful discussions. They also would like to acknowledge the courtesy of B. J. Carter who kindly sent the photograph shown in Figure 1. The work was supported by the US National Science Foundation (grants CMS-9896136 and OCE-0221974) and the US-Israel Binational Science Foundation (grant 9800135).

References

Atkinson, B. K., and P. G. Meredith (1987), Experimental fracture mechanics data for rocks and minerals, in *Fracture Mechanics of Rock*, edited by B. K. Atkinson, pp. 477–525, Academic, San Diego, Calif.

Bai, T., and D. D. Pollard (2001), Getting more for less: The unusual efficiency of fluid flow in fractures, *Geophys. Res. Lett.*, *28*, 65–68.

Bai, T., D. D. Pollard, and M. R. Gross (2000), Mechanical prediction of fracture aperture in layered rocks, *J. Geophys. Res.*, *105*, 707–721.

Barenblatt, G. I. (1962), The mathematical theory of equilibrium cracks in brittle fracture, *Adv. Appl. Mech.*, *7*, 55–129.

Ben Naceur, K., and J.-C. Roegiers (1990), Design of fracturing treatments in multilayered formations, *SPE Prod. Eng.*, *1990*, 21–26.

Bird, R., R. C. Armstrong, and O. Hassager (1987), *Dynamics of Polymeric Liquids*, vol. 1, *Fluid Mechanics*, John Wiley, Hoboken, N. J.

David, C. (1993), Geometry of flow paths for fluid transport in rocks, *J. Geophys. Res.*, *98*, 12,267–12,278.

Economides, M. J., and K. G. Nolte (Eds.) (2000), *Reservoir Stimulation*, 3rd ed., John Wiley, Hoboken, N. J.

Engelder, T., and A. Lacazette (1990), Natural hydraulic fracturing, in *International Symposium on Rock Joints*, edited by N. Barton and O. Stephansson, pp. 35–43, A. A. Balkema, Brookfield, Vt.

Engelder, T., and G. Oertel (1985), Correlation between abnormal pore pressure and tectonic jointing in the Devonian Catskill Delta, *Geology*, *13*, 863–866.

Engelder, T., P. Hagin, B. Haith, A. Lacazette, S. Loewy, D. McConaughy, and A. Younes (1999), The Catskill Delta Complex: Analog for modern continental shelf and delta sequences containing overpressured sections, Seal Eval. Consortium Field Trip, Penn. State Univ., University Park.

Gangi, A. F. (1978), Variation of whole and fractured porous rock permeability with confining pressure, *Int. J. Rock Mech. Mineral. Sci. Geomech. Abstr.*, *15*, 249–257.

Gavrilenko, P., and Y. Gueguen (1989), Pressure dependence of permeability: A model for cracked rocks, *Geophys. J. Int.*, *98*, 159–172.

Germanovich, L. N., and D. K. Astakhov (2004), Fracture closure in extension and mechanical interaction of parallel joints, *J. Geophys. Res.*, *109*, B02208, doi:10.1029/2002JB002131.

Germanovich, L. N., and R. P. Lowell (1992), Percolation theory, thermoelasticity, and discrete hydrothermal venting in the Earth's crust, *Science*, *225*, 1564–1567.

Germanovich, L. N., and R. P. Lowell (1995), The mechanism of phreatic eruptions, *J. Geophys. Res.*, *100*, 8417–8434.

Germanovich, L. N., D. K. Astakhov, J. Shlyapobersky, and L. M. Ring (1998), A model of hydraulic fracture with parallel segments, in *Modeling and Simulation Based Engineering*, edited by S. N. Atluri and P. E. O'Donoghue, pp. 1261–1268, Tech Sci. Press, Encino, Calif.

Germanovich, L. N., R. P. Lowell, and D. K. Astakhov (2000), Stress-dependent permeability and the formation of seafloor event plumes, *J. Geophys. Res.*, *105*, 8341–8354.

Germanovich, L. N., R. P. Lowell, and D. K. Astakhov (2001), Temperature-dependent permeability and bifurcations in hydrothermal flow, *J. Geophys. Res.*, *106*, 473–495.

Gidley, J. L., S. A. Holditch, D. E. Nierode, and R. W. Veatch Jr. (Eds.) (1989), *Recent Advances in Hydraulic Fracturing*, 452 pp., Soc. of Petrol. Eng., Richardson, Tex.

Gradshteyn, I. S., and I. M. Ryzhik (2000), *Table of Integrals, Series, and Products*, 6th ed., edited by A. Jeffrey and D. Zwillinger, Academic, San Diego, Calif.

Helgeson, D. E., and A. Aydin (1991), Characteristics of joint propagation across layer interfaces in sedimentary rocks, *J. Struct. Geol.*, *13*, 897–911.

Ji, S., and K. Saruwatari (1998), A revised model for the relationship between joint spacing and layer thickness, *J. Struct. Geol.*, *20*, 1495–1508.

Jones, F. O. (1975), A laboratory study of the effects of confining pressure on flow and storage capacity in carbonate rocks, *J. Petrol. Technol.*, *1975*, 21–27, Jan.

Kranz, R. L., A. D. Frankel, T. Engelder, and C. H. Scholz (1979), The permeability of whole and jointed Barre granite, *Int. J. Rock Mech. Mineral. Sci. Geomech. Abstr.*, *16*, 225–235.

Long, J. C. S., et al. (1996), *Rock Fractures and Fluid Flow, Contemporary Understanding and Applications*, 551 pp., Natl. Acad. Press, Washington, D. C.

Lowell, R. P., and L. N. Germanovich (1995), Dike injection and the formation of megaplumes at ocean ridges, *Science*, *267*, 1804–1807.

Lowell, R. P., P. Van Cappellen, and L. N. Germanovich (1993), Silica precipitation in fractures and the evolution of permeability in hydrothermal upflow zones, *Science*, *260*, 192–194.

Mahrer, K. D., W. W. Aud, and J. T. Hansen (1996), Far-field hydraulic fracture geometry: A changing paradigm, paper presented at 1996 SPE Annual Technical Conference and Exhibition, Denver, Colo., Soc. of Petrol. Eng., Richardson, Tex., 6–9 Oct.

Martin, J. T., and R. P. Lowell (2000), Precipitation of quartz during high-temperature fracture-controlled hydrothermal upflow at ocean ridges: Equilibrium versus linear kinetics, *J. Geophys. Res.*, *105*(B1), 869–882.

Neuzil, C. E., and J. V. Tracy (1981), Flow through fractures, *Water Resour. Res.*, *17*, 191–199.

Nolte, K. G. (1987), Discussion of influence of geologic discontinuities on hydraulic fracture propagation, *J. Petrol. Technol.*, *1987*, 998.

Oron, A. P., and B. Berkowitz (1998), Flow in rock fractures: The local cubic law assumption reexamined, *Water Resour. Res.*, *11*, 2811–2825.

Pyrak-Nolte, L. J., N. G. W. Cook, and D. D. Nolte (1988), Fluid percolation through single fractures, *Geophys. Res. Lett.*, *5*, 1247–1250.

Raven, K. G., and J. E. Gale (1985), Water flow in a natural rock fracture as a function of stress and sample size, *Int. J. Rock Mech. Mineral. Sci. Geomech. Abstr.*, *22*, 251–261.

Renshaw, C. E., and D. D. Pollard (1995), An experimentally verified criterion for propagation across unbounded frictional interfaces in brittle, linear elastic materials, *Int. J. Rock Mech. Mineral. Sci. Geomech. Abstr.*, *32*, 237–249.

Sisavath, S., and R. W. Zimmerman (2000), A simple model for deviations from the "cubical law" for a fracture under normal stresses, paper presented at 3rd Euroconference on Rock Physics and Rock Mechanics, Univ. of Bonn, Bad Honnef, Germany.

Srivastava, D. C., and T. Engelder (1991), Fluid evolution history of brittle-ductile shear zones on the hanging wall of Yellow Spring thrust, Valley and ridge province, Pennsylvania, USA, *Tectonophysics*, *198*, 23–34.

Tada, H., P. C. Paris, and G. R. Irwin (1985), *The Stress Analysis of Cracks Handbook*, Paris Production, Inc., Del Res. Corp., St. Louis, Missouri.

Tsang, Y. W., and P. A. Witherspoon (1981), Hydromechanical behavior of a deformable rock fracture subject to normal stress, *J. Geophys. Res.*, *86*, 9287–9298.

Vermilye, J. M., and C. H. Scholz (1995), Relation between vein length and aperture, *J. Struct. Geol.*, *17*, 423–434.

Waite, M. E., S. Ge, and H. Spetzler (1999), A new conceptual model for fluid flow in discrete fractures: An experimental and numerical study, *J. Geophys. Res.*, *104*, 13,049–13,059.

Walsh, J. B. (1981), Effect of pore pressure and confining pressure on fracture permeability, *Int. J. Rock Mech. Mineral. Sci. Geomech. Abstr.*, *18*, 429–435.

Witherspoon, P. A., J. S. Wang, K. Iwai, and J. E. Gale (1980), Validity of cubic law for fluid flow in a deformable rock fracture, *Water Resour. Res.*, *16*, 1016–1024.

D. K. Astakhov, Pinnacle Technologies, Inc., Bakersfield, CA 93309-0654, USA.

L. N. Germanovich, School of Civil and Environmental Engineering, Georgia Institute of Technology, Atlanta, GA 30332-0355, USA. (leonid@ce.gatech.edu)